Volume 135 July 2014 ISSN 0924-7963

Special Issue
Assessing and modelling ecosystem changes in the Mediterranean and the
Black Sea pelagic ecosystem - SESAME

Edited by
Marilaure Gregoire
Javier Ruiz
Emin Özsoy
Evangelos Papathanassiou

JOURNAL OF
MARINE
SYSTEMS

Journal of Marine Systems 135 (2014) 29–43

Contents lists available at ScienceDirect

Journal of Marine Systems

journal homepage: www.elsevier.com/locate/jmarsys

Spatial and temporal variability in the chemical properties of the oxic and suboxic layers of the Black Sea

Süleyman Tuğrul [a,*], James W. Murray [b], Gernot E. Friederich [c], İlkay Salihoğlu [a,1]

[a] *Middle East Technical University, Institute of Marine Sciences, Erdemli, Mersin, Turkey*
[b] *School of Oceanography, University of Washington, Seattle, WA 98195-5351, USA*
[c] *MBARI, 7700 Sandholdt Rd., Moss Landing, CA 95039, USA*

ARTICLE INFO

Article history:
Received 28 January 2012
Received in revised form 7 August 2013
Accepted 2 September 2013
Available online 21 September 2013

Keywords:
Nutrients
Oxygen
Dissolved manganese
Suboxic
Anoxic
Black Sea

ABSTRACT

The Black Sea, a land-locked deep basin with sulfide bearing waters below 150–200 m, has been subject to anthropogenic pressures since the 1970s. Large inputs of nutrients (nitrate — N, phosphate — P, silicate — Si) with high N/P but low Si/N ratios and subsequent development of intensive eutrophication over the basin have changed vertical distributions and inventories of nutrients and redox-sensitive metals in the oxic, suboxic and anoxic layers. Chemical data sets obtained between 1988 and 2010, and older data from before 1970 were evaluated to assess spatial/temporal variations of the dissolved oxygen (O_2), nutrients and dissolved/particulate manganese (Mn_d, Mn_p) in the water column from the lower salinity, oxygenated surface waters through the SubOxic Layer (SOL; $O_2 < 20$ μM; $H_2S < 1$ μM) to the anoxic, sulfidic water interface. Correlations were observed between salinity and nutrients (nitrate, silicate) in the nearshore waters off the Danube delta and in the southwestern (SW) coastal waters which had low Si/N ratios. Surface waters from the western central gyre were consistently depleted in nitrate and phosphate with low N/P but higher Si/N molar ratios throughout the year. Chemical profiles obtained recently in the Rim Current and western central gyre displayed very similar vertical features through the halocline to the sulfidic water interface. However, in the SW coastal margin, lateral intrusion of O_2 and nutrients by the Bosporus Plume resulted in formation of secondary maxima of nitrate, nitrite and O_2 in the SOL, and local deepening of the first appearance of anoxic, sulfidic waters. Before the mid 1960s, nitrate-enriched major rivers fed the Black Sea with high N/P ratios (>50). The surface waters over the basin were rich in silicate (25–70 μM), but poor in nitrate (<0.1 μM) and phosphate (0.05–0.3 μM), resulting in very high Si/N (>500) but very low N/P (<1.0) ratios. After the mid 1970s, construction of dams, especially on the Danube River, resulted in lower Si concentrations. At this time the increased loads of anthropogenic nitrate and phosphate by the major rivers resulted in lower Si/N, but still high N/P molar ratios, which enhanced eutrophication (production of particulate organic matter, POM) drastically in the coastal waters. This led to reductions in the surface Si/N ratio by up to 500-fold in the western basin while the N/P ratio increased. The enhanced POM export increased the nitrate inventory and thus N/P ratios of the NW shelf waters spreading over the whole basin. The increased export of POM decreased the Si inventory of the upper layer down to the boundary of sulfidic waters. This export also increased O_2 consumption and removal of nitrate to N_2 form by denitrification in the oxic/suboxic interface, leading to seasonal/decadal changes in the boundaries of the nitracline and main oxycline and changes in the slopes of the nitrate-phosphate and Apparent Oxygen Utilization (AOU)-nitrate regressions in the steep oxycline down to the SOL. These slopes are much smaller than those observed in the lower layer of Marmara Sea fed by the Black Sea outflow. The enlargement of SOL by ~15–20 m after the 1970s modified the vertical features of nitrate, phosphate and manganese (Mn_d, Mn_p) species in the redox gradient zone.

1. Introduction

The Black Sea provides an excellent site to study biogeochemical distributions and microbially mediated reactions under oxic, suboxic and anoxic (sulfidic) conditions in the water column (Murray et al., 1995). The reason why these conditions exist is that the Black Sea is strongly stratified with a surface layer of low salinity (S ~ 17–18) due to large riverine input of fresh water (Sorokin, 2002) (Fig. 1). The only source of salty water is from the Mediterranean through the Bosporus Strait via the Sea of Marmara. As a result there is a strong salinity-driven density gradient and a permanent halocline which limits vertical supply from the deeper layers (Brewer and Murray, 1973; Konovalov and Murray, 2001; Oguz, 2002). In winter, however, limited exchanges of dissolved oxygen (O_2) and nutrients occur between the surface layer

---

[*] Corresponding author. Fax: +90 324 5212327.
E-mail address: tugrul@ims.metu.edu.tr (S. Tuğrul).

[1] Present address: Near East University, Nicosia, Northern Cyprus, Cyprus.

0924-7963/$ – see front matter © 2013 Elsevier B.V. All rights reserved.
http://dx.doi.org/10.1016/j.jmarsys.2013.09.008

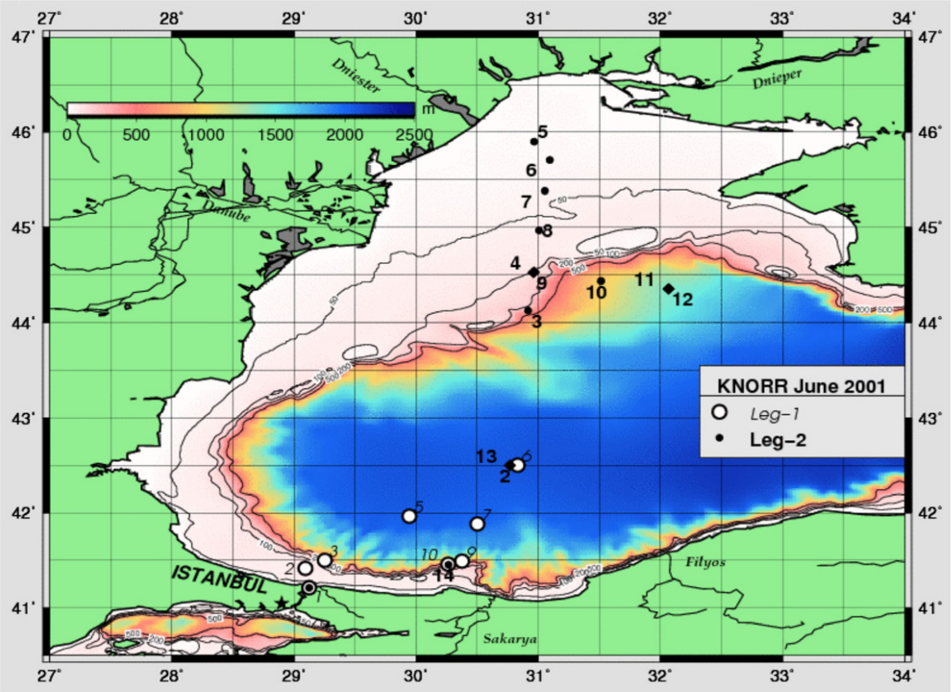

Fig. 1. Location of sampling stations in the western Black Sea visited during the first (L-1) and second (L-2) legs of the May–June 2001 R/V Knorr cruise (note: four stations were visited twice).

and the upper depths of the permanent halocline by deeper mixing (e.g. Gregg and Yakushev, 2005; Oguz, 2002). This has resulted in permanent anoxia in the subhalocline waters below 125–200 m over most of the basin (Oguz, 2008). At the boundary between the oxic surface and sulfidic deep waters there is a layer with essentially no oxygen (<20 μM) or sulfide (<1.0 μM) referred to as the SubOxic Layer (SOL) (Murray et al., 1995; Tugrul et al., 1992).

The distributions of hydro-chemical properties in the upper layer appear to be sensitive to external pressures originating from climate variability (Konovalov and Murray, 2001; Oguz and Velikova, 2010) and anthropogenic inputs (Kıdeyş, 2002; Mee, 1992; Oguz, 2008). These distributions are influenced by the surface circulation, which is dominated by basin wide cyclonic currents, leading to formation of two quasi-permanent cyclones or gyres in the interiors of the eastern and western basins and a series of anticyclonic eddies within the Rim Current along the coastal margin (Oguz et al., 1992; Ozsoy et al., 1993). There is a temperature minimum water layer called the Cold Intermediate Layer (CIL) located at about 50 m that originates in the winter on the northwest (NW) shelf (Tolmazin, 1985) and (at least in some severe winters) in the western central gyres (Gregg and Yakushev, 2005). The dense, high salinity (S ~ 38) water from the Bosporus outflow mixes with the overlying CIL on the SW shelf (Latif et al., 1991; Murray et al., 1991) and the resulting mixture produces lateral injections of what is referred to as the Bosporus Plume (Konovalov et al., 2003; Ozsoy et al., 1993). All deep water falls along a quasi-linear T–S relation connecting the low-Temperature CIL with the high-salinity Bosporus end-member, modified primarily by climate driven variability in the T–S properties of the CIL. The depths of these lateral intrusions vary depending on the mixing conditions on the shelf but they ultimately ventilate all depths below the CIL. They are the only sources of salt and O_2 to the subhalocline waters of the Black Sea. The Bosporus Plume injects oxygenated (200–250 μM) water into the pycnocline, which results in complicated vertical distributions in the SW region of the basin (Fuchsman et al., 2012; Konovalov et al., 2003). These lateral fluxes of O_2, together with the redox reactions of manganese in the redox gradient zone (Glazer et al., 2006; Trouwborst et al., 2006; Yakushev et al., 2009), keep the sulfidic (≥1 μM) waters at a fairly stable and constant density over the deep basin (Konovalov and Murray, 2001; Konovalov et al., 2003, 2005; Murray et al., 1995; Tugrul et al., 1992).

It has been documented that various biogeochemical distributions are associated with characteristic density values in the Black Sea (Tugrul et al., 1992; Murray et al., 1995; Vinogradov and Nalbandov, 1990). Because these density surfaces vary with depth (because of the surface circulation patterns) it is most convenient to use density as the depth coordinate rather than depth itself (Figs. 2–3). This provides a unifying approach for comparing and analyzing data from different locations in different years.

In the absence of upwelled nutrients, new production in the Black Sea is dominated by nutrient inputs from the major rivers and precipitation during the spring-autumn period (Cociasu et al., 1996; Medinets and Medinets, 2012; Yayla et al., 2001). There have been several reports suggesting that changes in river inputs of nutrients with modified nitrate/phosphate/silicate (N/P/Si) molar ratios have influenced both biological and chemical properties of the whole Black Sea, but especially the wide NW shelf region (Cociasu et al., 1996; Kıdeyş, 2002; Yunev et al., 2002). These alterations to the chemical inventories and marine ecosystem first occurred in the 1970s on the wide NW shelf, which directly receives the inputs of pollutants by the three main rivers (mainly the Danube but also the Dnieper and Dniester, with a total discharge of 260 km^3/y) (Berlinski et al., 2003; Cociasu et al., 1996; Kıdeys, 2002; Mee, 1992; Mee et al., 2005; Oguz et al., 2008). The inventory of nitrate in the oxic and suboxic waters became enhanced by 2–4 times to ~250 mmol m^{-2} in the central basin, while the silicate inventory exhibited a decreasing trend (Codispoti et al., 1991; Konovalov and Murray, 2001; Tugrul et al., 1992). The effects of eutrophication on the nutrient and sulfide inventories of the Black Sea and decadal changes in the chemistry of the oxic/anoxic transition zone were evaluated by Konovalov and Murray (2001). The SOL appeared to become enlarged by ~15–20 m in the central gyre (Basturk et al., 1998; Konovalov et al., 2005; Murray et al.,

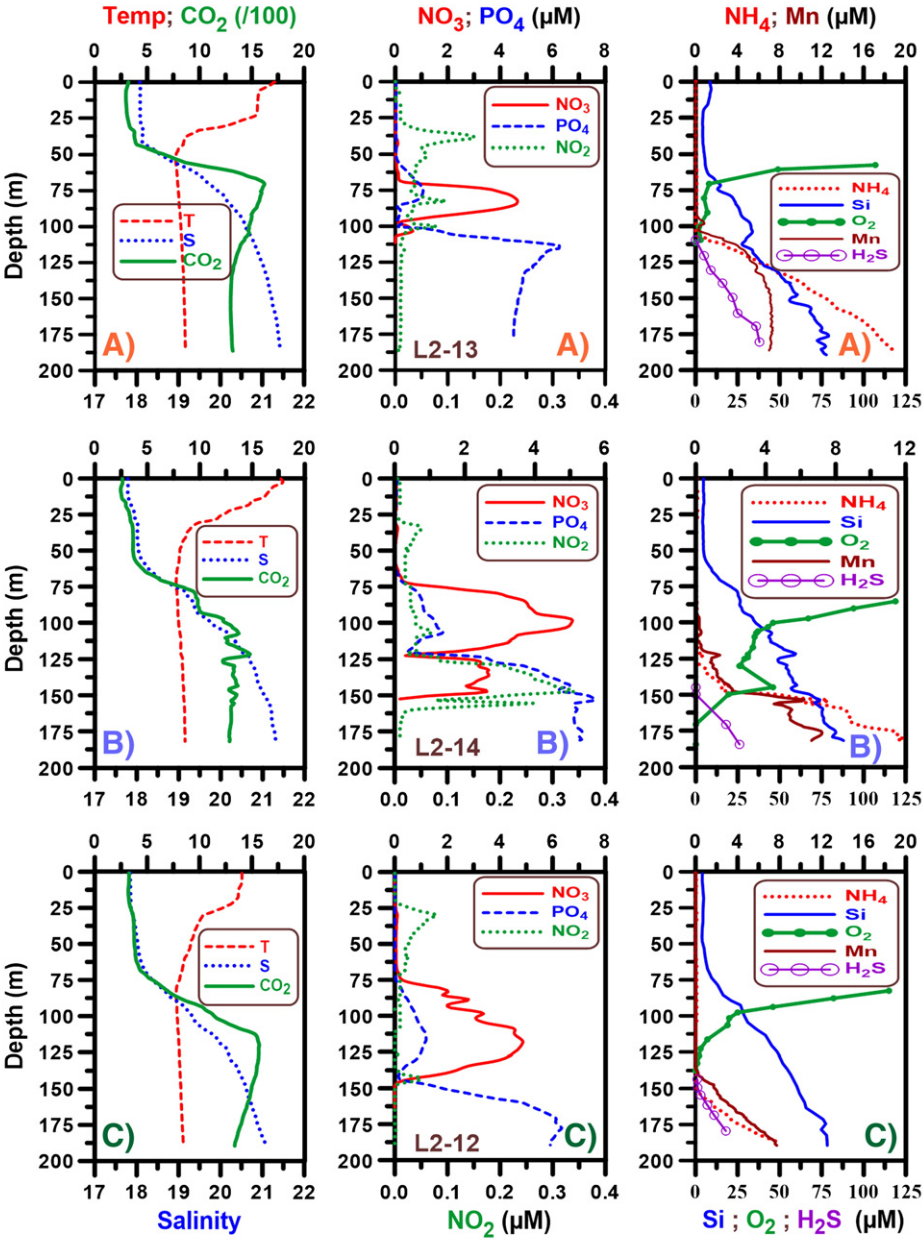

Fig. 2. Typical depth profiles of pump-cast hydro-chemical data obtained in (A): the central western gyre (L2–3), (B): the southwestern (SW) coastal region (L2–14) and (C): the north-western (NW) slope (L2–12) in the early June 2001 (data with symbols are from bottle-cast).

1989; Tugrul et al., 1992). Eutrophication may also impact the roles of manganese (Mn_d, Mn_p) cycling on the formation of the deep phosphate minimum in the redox boundary ($O_2 < 5.0$ μM) (Trouwborst et al., 2006; Yakushev et al., 2009). The first integrated biogeochemical studies of the Black Sea were carried out during the US–Turkish Black Sea Expedition on the R/V Knorr in 1988 (Murray and Izdar, 1989). The Knorr 1988 data sets included high-resolution profiles of nutrients and dissolved manganese and iron using both a pump-profiling system and CTD-rosette bottle-casts. We had an opportunity to address some of the questions that came from the 1988 Expedition using similar sampling approaches during another R/V Knorr cruise in 2001. In this paper we report the data from R/V Knorr 2001. Comparison of these data with data from R/V Knorr 1988 and 2003, R/V Bilim multi-cruises (1987–2010), R/V Parshin 2005, R/V Endeavor 2005 and other historical data sets (such as Atlantis II 1969) will be used to examine regional and temporal variability in vertical distributions of nutrients and manganese in the western Black Sea and the impact of lateral intrusions from the Bosporus Plume.

2. Methods

The R/V Knorr 2001 cruise had two legs in the western Black Sea and was conducted from 20 May to 10 June, 2001. The locations of stations occupied during Leg 1 and Leg 2 are shown in Fig. 1. Other data sets used in this study were obtained from the R/V Knorr 1988 (Codispoti et al., 1991), R/V Parshin 2005 and R/V Bilim multicruises by Middle East Technical University — Institute of Marine Sciences (METU-IMS) between 1987 and 2010. Historical data were obtained from the technical report of the R/V Atlantis II cruise in 1969 (Brewer, 1971) and from the Black Sea Oceanographic Database (BSOD) created in framework of NATO Linkage (Grant number: 980494). Water samples for chemical analyses from the R/V Knorr, R/V Parshin and R/V Bilim cruises were collected using General Oceanic Go-Flo bottles attached to a rosette — CTD (conductivity, temperature, depth). Dissolved inorganic nutrients (nitrate, nitrite, ammonia, reactive phosphate and silicate with detection limits of 0.02, 0.005, 0.05, 0.02, 0.1 μM, respectively), dissolved manganese (Mn_d) and iron (Fe^{+2}) were measured using a 6-channel Technicon model AAII auto-analyzer. Automated methods for dissolved Mn and Fe (detection limits: 0.04 and 0.005 μM) used in this study were adapted from the manual methods given in Grasshoff et al. (1983). The silicate channel was replaced by Fe at selected pump-cast stations. For precise analyses of nutrient-poor euphotic zone waters, bottle-cast samples were analyzed separately at high sensitive modes of the automated system. In addition to bottle casts, pump-cast profiles were obtained during the Knorr 1988 and 2001 cruises by coupling the six sampling lines of the auto-analyzer to the outlet of CTD-coupled pump-profiling system (200 m long tubing) on deck. The depth resolution was less than 2 m (Codispoti et al., 1991). The start time of multi-channel analyses was recorded when the CTD was at the surface and the automated analyses were terminated after the CTD was kept at about 190 m for at least 4–5 min to reach a plateau at the end of each chemical profile. The nitrate sample line was removed from the outlet when the baseline concentrations were reached within the sulfidic interface (H_2S > 1 μM). This depth was always recorded to fit the nitrate profile to CTD and other chemical data. After completion of the pump profiles and return to stable baselines for all channels, standards prepared in nutrient-poor surface seawater were run under the same analytical condition to determine the calibration slopes precisely for each parameter. Unfiltered dissolved Mn profiles were recalibrated, using the results of filtered Mn_d samples from bottle casts (Yemenicioğlu et al., 2006). The measurements of O_2 and sulfide were carried out by the automated Winkler titration and

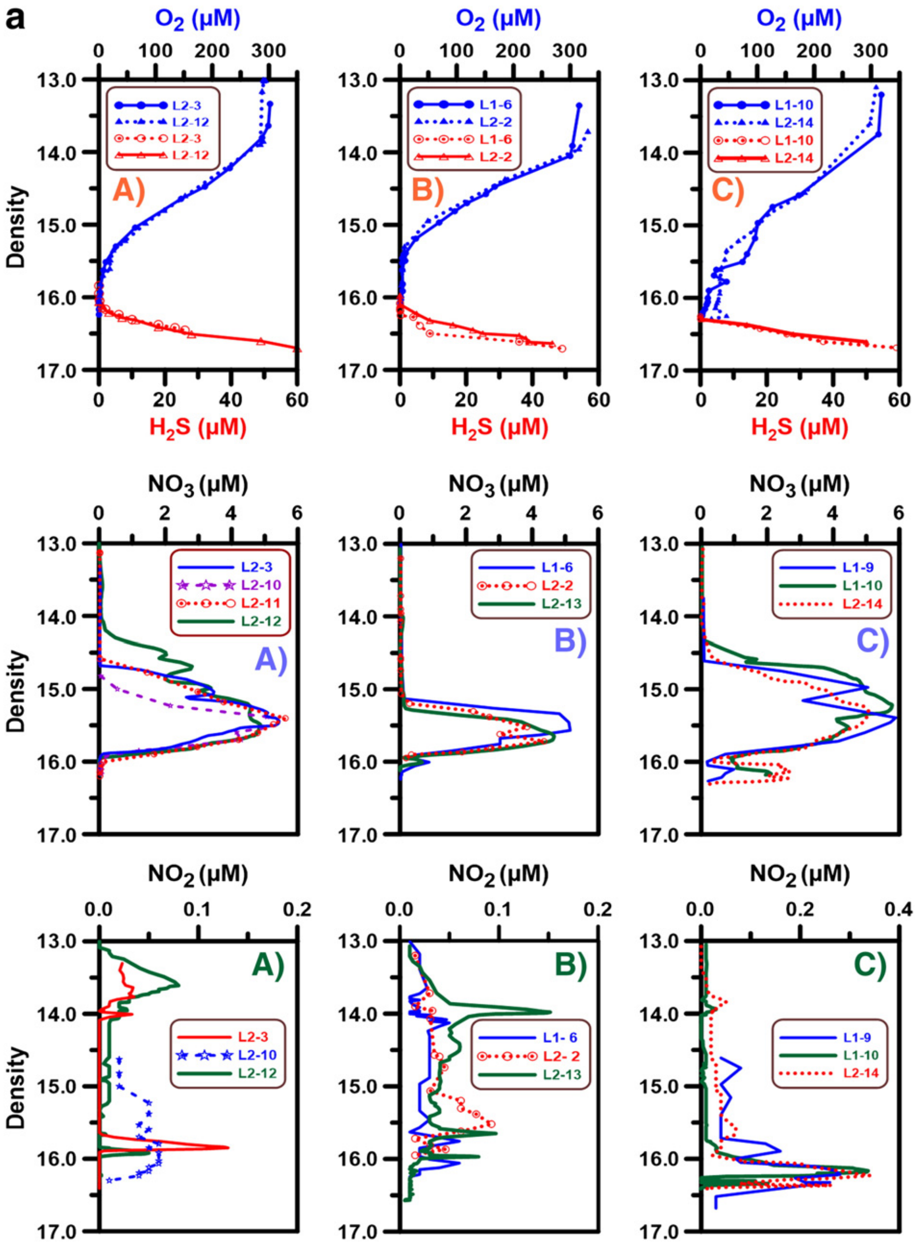

Fig. 3. a. Representative profiles versus density of dissolved oxygen, hydrogen sulfide, nitrate and nitrite from the northern slope (A), central western gyre (B) and the southwestern coastal region (C) in late May–June 2001 (data with symbols are from bottle-cast). b. Representative profiles versus density of phosphate, silicate, ammonia, dissolved manganese (Mn) and reduced iron (Fe) in the northwestern slope (A), central western gyre (B) and southwestern coastal region (C) in the late May–June 2001 (data with symbols are from bottle-cast).

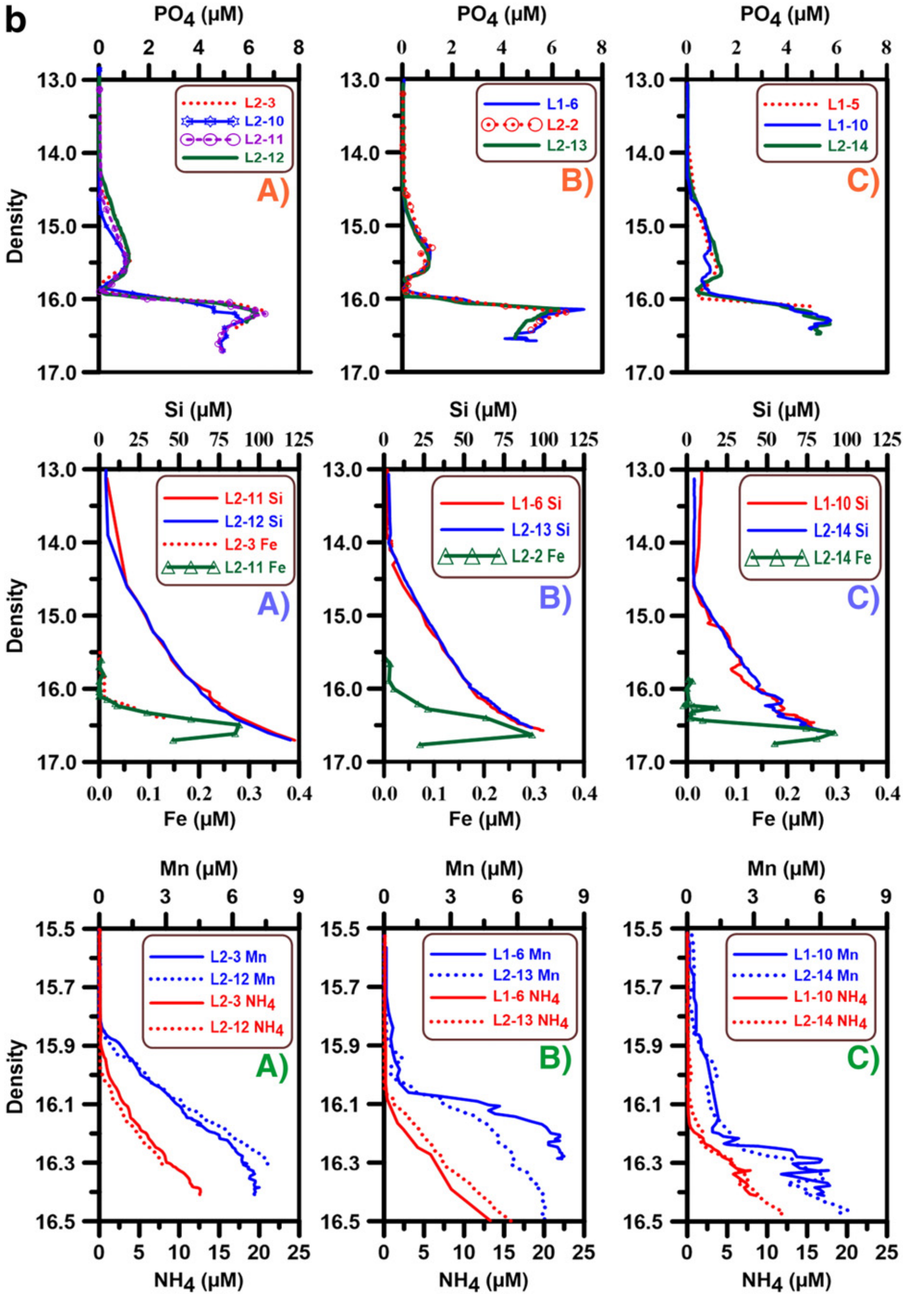

Fig. 3 (*continued*).

manual colorimetric method at a low concentration range (detection limits: 3.0 and 0.1 µM, respectively) (Grasshoff et al., 1983).

3. Results

We evaluated data sets from bottle and pump casts obtained during the Knorr cruise in June 2001 to the NW shelf, slope, central basin and SW rim current (Fig. 1). Concentrations of dissolved inorganic nutrients, manganese and iron (Mn_d and Fe^{+2}) were very low in the low salinity mixed layer (15–20 m deep) throughout the basin. The mixed layer concentrations were as low as 0.04–0.1 µM for nitrate (including nearly undetectable nitrite values of 0.01–0.03 µM) and 0.02–0.04 µM for phosphate. Surface silicate concentrations, however, were more variable and consistently higher in the coastal regions due to riverine input, then decreased from 4–9 µM on the shelf to 1–4 µM in the central gyre ($S > 18.0$). In the oxic/anoxic transition layer found in the permanent pycnocline below the oxygenated surface water, depth distributions of nutrients (N, P) and redox-dependent trace metals displayed distinct vertical features throughout the basin (Fig. 2) These chemical features were located in the permanent halocline which deepened from the central basin to the Rim Current and anticyclonic eddies in the coastal areas. Intrusions of the warm, salty Bosporus Plume modified the chemical distributions in the SW Black Sea. Therefore, depth of the nutrients, O_2 and redox-sensitive trace metals (Mn_d, Fe^{2+}) from the Knorr-2001 cruise (Fig. 1) are evaluated regionally to focus on processes influencing formation and persistence of principal chemical properties of the oxic and suboxic layer in each region (Figs. 2–3). Density (sigma-t, σ_t) dependent composite profiles from the SW, central gyre and NW shelf/slope regions (Fig. 3) are also used to evaluate spatial variability in chemical features.

3.1. West-central basin

Typical depth and density profiles of hydro-chemical parameters obtained at Station 13 of Leg 2 (Fig. 1) within the western gyre on 8 June 2001 are shown in Figs. 2–3. O_2 concentrations decreased steeply in the oxycline from saturated levels (>300 μM at 30–35 m) in the mixed layer to suboxic concentrations (<20 μM) at 70 m (Fig. 2). The lower boundary of the oxycline defines the upper boundary (O_2 ~ 20 μM) of the SOL where O_2 decreased gradually to undetectable levels (<3 μM) below 100 m, corresponding to the sigma-t (σ_t) ~ 16.0 surface in Fig. 3. Sulfide became detectable (>1.0 μM) at ~115 m where σ_t ~ 16.15–16.2. In June 2001 the nitrate-depleted surface layer unexpectedly extended down to the base of the main oxycline at 65–70 m. The nitrate maximum was located at the top of the SOL (O_2 < 20 μM), reaching a maximum of 5.0 μM at about 85 m. Nitrate then decreased steeply to 0.1 μM at ~95 m where O_2 < 5 μM and σ_t ~ 15.95. At this location in the gyre, it increased again slightly at ~100 m within the suboxic/anoxic interface, resulting in a secondary maximum which coincided with the small nitrite peak in the continuous profiles (clearly seen in Figs. 2–3). The silicate profile displayed the opposite changes, indicating lateral intrusions of rim current waters with different chemical properties. This type of chemical feature could not be detected in the bottle cast profiles due to their low resolution sampling intervals. Nitrite concentrations were very low in the surface layer; nevertheless, detectable peaks due to nitrification were recorded at the base of the mixed layer where photosynthetic activity had almost vanished. Small nitrite maxima were also situated within the nitrate maximum (due to nitrification) and in the suboxic/anoxic transition zone (due to denitrification). The ammonium concentrations started to increase within the anoxic interface at about 105 m (where σ_t ~ 16.0 in Fig. 3), and then increased steadily with depth in the sulfidic deep water. Concentrations of nitrate and ammonium decrease essentially to zero (<0.1 μM) between 95 and 105 m. Phosphate profiles displayed a broad maximum within the upper depths of the SOL below 65 m, followed by an intense minimum of 0.05–0.1 μM between 85 and 95 m where O_2 ~ 5.0 μM (σ_t:15.8–15.9 in Fig. 3); then, the concentrations increased sharply to form the deep P-maximum at the sulfidic water boundary. The silicate profile was very similar to that of salinity; the gradient commenced at the halocline boundary (~45 m), and concentrations increased steadily down to subhalocline depths. The onset of increasing Mn_d was situated within the suboxic/anoxic interface at nearly 100 m (where nitrate had almost vanished) and then increased slightly with depth in the upper anoxic waters.

3.2. Southwestern (SW) coastal region

Typical depth profiles of nutrients, oxygen and Mn_d, which display characteristic features in the oxic/anoxic transition zone, were modified due to the intrusion of the oxygenated, nitrate-rich Bosporus Plume into the halocline depths of the SW Black Sea (St. 14 in Fig. 2). The nutricline coincided exactly with the oxycline in the upper halocline over basin, but appeared at greater depths and broader in the coastal regions and Rim Current (Basturk et al., 1998; Codispoti et al., 1991; Oguz, 2002). Below the low nutrient upper layer of ~60 m, the nutrient concentrations remained low in the CIL waters. As shown in Fig. 2, the chemocline commenced at about 65–70 m in the SW Rim Current. Nitrate increased markedly from 0.1 μM at 70 m to a broad maximum of 5–5.5 μM at 105–110 m (between σ_t ~ 15.35–15.45 in Fig. 3), within the oxic/suboxic transition zone (O_2 < 50 μM). Phosphate profiles displayed gradual increases with depth from the oxycline to the SOL, followed by a weaker deep minimum and then a deeper maximum at greater depths in the anoxic, sulfidic water interface (Fig. 2); these features were slightly influenced by the Bosporus Plume. In June 2001, below the nitrate maximum, the nitrate concentrations decreased steeply down to 125 m, which was within the O_2-depleted layer (~25–50 μM) and then increased again to about 2 μM and formed a homogeneous layer about 25 m thick between 125 and 150 m (between σ_t: 16.0–16.3 in Fig. 3). Nitrate then decreased to zero in the anoxic interface below 150 m. This secondary broad nitrate peak coincided with the appearance of a similar nitrite feature in the lower depth of the suboxic zone (Fig. 2), where the O_2 profile also exhibited a small maximum. Small minima and maxima were also seen in the profiles of dissolved CO_2, Mn, silicate and ammonium.

3.3. Northwestern (NW) slope region

Typical pump-cast profiles, obtained at St. 12 on the NW slope, were very similar to those in the west-central gyre (Fig. 2). The main oxycline extended to 120–125 m where nitrate and phosphate displayed maxima. The upper nitracline, which coincided with the oxycline, was situated between 75 and 125 m (σ_t = 14.2–15.4 in Fig. 3). However, the nitrate profile did display some undulating patterns with small maxima between 75 and 100 m where the gradients of O_2, CO_2 and silicate concentrations also changed slightly. Nitrite concentrations were very low in the water column, ranging from 0.01 to 0.1 μM, exhibiting two small maxima at the base of the euphotic zone and in the suboxic layer. The onsets of increasing Mn_d and ammonia concentrations were situated sequentially between 135 and 150 m where O_2 < 10 μM in the SOL. A deep phosphate minimum at ~140 m, which coincided with the onset of increasing Mn_d, was similar to that seen in the central gyre. The deeper phosphate maximum was also

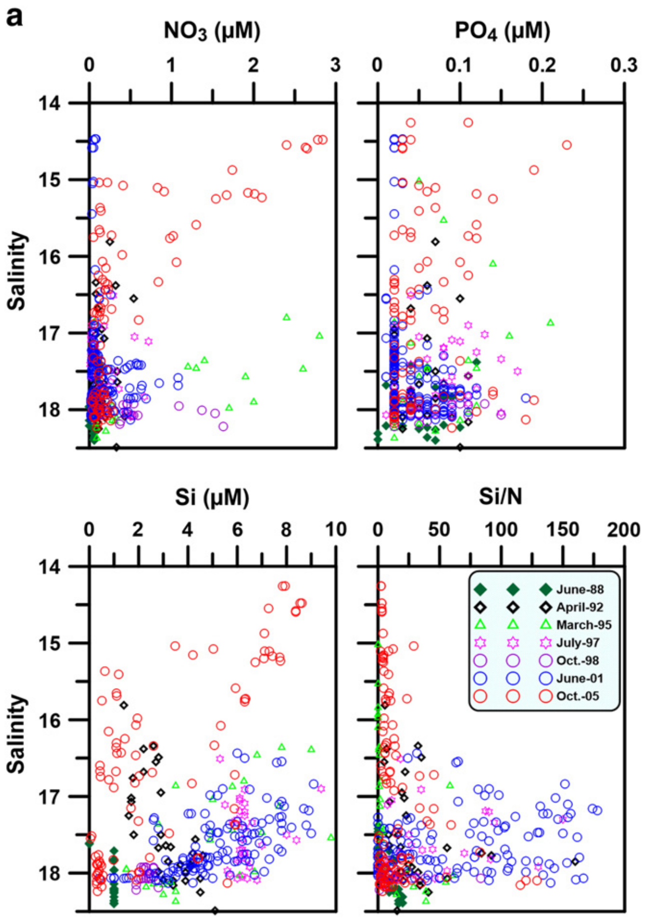

Fig. 4. a. Salinity-dependent distributions of silicate, phosphate, nitrate and silicate/nitrate ratios in surface waters (0–10 m) of the NW shelf and SW Rim Current between1988 and 2005. b. Surface distributions of nitrate + nitrite and silicate (Si) concentrations in the western Black Sea in late March–April 1995 and October 2005. c. Variations of nutrients (nitrate + nitrite, phosphate, silicate), their molar ratios (N/P, Si/N) in the near-surface (0–10 m; but 0–25 m for the Atlantis 1969 data) of the western central gyre (A: upper panel) and SW Rim Current (B: lower panel).

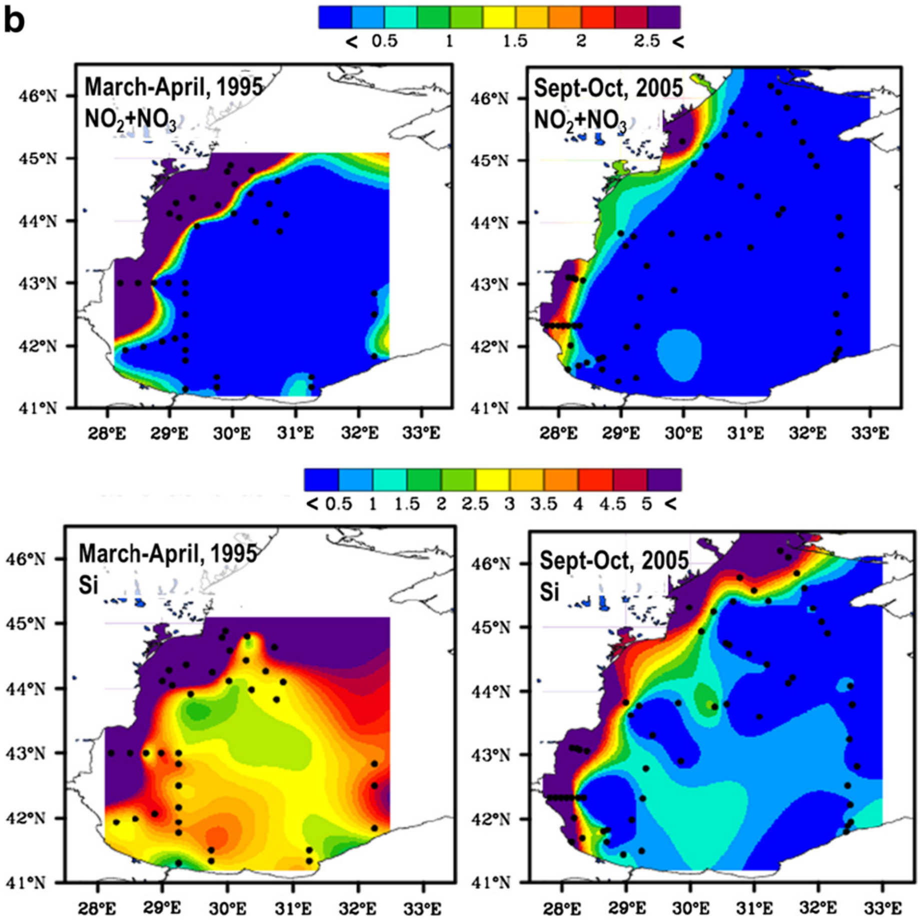

Fig. 4 (*continued*).

situated at the sulfide interface. As shown in Figs. 2 and 3, the undulating vertical features of nitrate and silicate observed between 70 and 110 m ($\sigma_t = 14.2$–15.2 in Fig. 3) suggest the occurrence of lateral mixing along the Rim Current and intrusion of shelf waters with the appropriate densities and different chemical properties to the interior basin waters.

4. Discussion

The formation of a seasonal thermocline in the surface layer and the presence of a strong halocline formed just below the CIL limits vertical exchanges with the deep waters, resulting in the formation of chemocline and SOL in the permanent halocline (Brewer and Murray, 1973; Konovalov and Murray, 2001; Oguz, 2002) Therefore, new production in the surface layer is dominated by nutrient inputs from the major rivers and precipitation during the spring–autumn period (Cociasu et al., 1996; Medinets and Medinets, 2012; Yayla et al., 2001). Starting the late 1970s, nutrient loads of the major rivers increased by 3–5 fold in the 1980s (~600–700 kton of nitrate-N and about 40 kton of P annually, Cociasu et al., 1996; Strokal and Kroeze, 2013) and precipitation (DIN ~ 300 kton y^{-1}, Medinets and Medinets, 2012) led to enhanced eutrophication in the upper layer waters over the basin (Konovalov and Murray, 2001; Mee, 1992; Mee et al., 2005). This enhanced eutrophication dramatically increased particulate organic matter (POM) production (equivalent to a net PON production of ~9×10^6 tons y^{-1}) and export below the euphotic zone. The majority of POM input has been decomposed in the strong halocline of the Rim Current and central basin by aerobic respiration (Karl and Knauer, 1991), resulting in significant spatial and temporal changes in the distinct chemical features driven by export production (Konovalov and Murray, 2001). We here discuss spatial and long-term impacts of the increased nutrient inputs on their surface distributions (using March–April 1995 and June 2001 data sets) and density-dependent vertical distributions of nutrients, O_2, manganese (Mn_d, Mn_p) and, inventories and molar (Si/N/P) ratios of nutrients in the oxygenated surface layer, the SOL and the anoxic, sulfidic layer interface of the west central basin and Rim Current.

4.1. Spatial variability in chemical features of the oxic-suboxic layers

Significant regional variations in the depths and density surfaces of the chemical features located in the permanent halocline were observed in the SW Rim Current and west central basin (Figs. 2–3). These differences result from various processes which include the circulation patterns and vertical mixing process (Oguz, 2002; Stanev and Becker, 1999), the intensity of shelf-basin interactions (Ginsburg et al., 2002; Gregoire and Friederich, 2004), nutrient inputs from major rivers (Oguz et al., 2008), fluxes of labile POM exported from the euphotic zone (Karl and Knauer, 1991) and ventilation by the oxygenated Bosporus Plume (Glazer et al., 2006; Konovalov et al., 2003; Ozsoy et al., 1993). The CIL formed in the upper halocline is a prominent feature with a core density of σ_t ~ 14.3–14.5 (at ~50 m) in the central gyre (Fig. 2). The CIL is replenished by variable, climate driven, inputs from the NW shelf (Konovalov and Murray, 2001; Oguz et al., 2006; Tolmazin, 1985) and by local vertical mixing during severe winters (Gregg and Yakushev, 2005). Thus, climatic changes in the depth and temperature of the CIL reflect spatial and temporal alterations in ventilation of the upper halocline (Glazer et al., 2006; Gregg and Yakushev, 2005; Oguz, 2008).

The oxygenated, less saline surface water layer extending down to the upper CIL defines the upper boundary of the oxycline (Figs. 2–3), which deepens in winter by deeper vertical mixing (Basturk et al.,

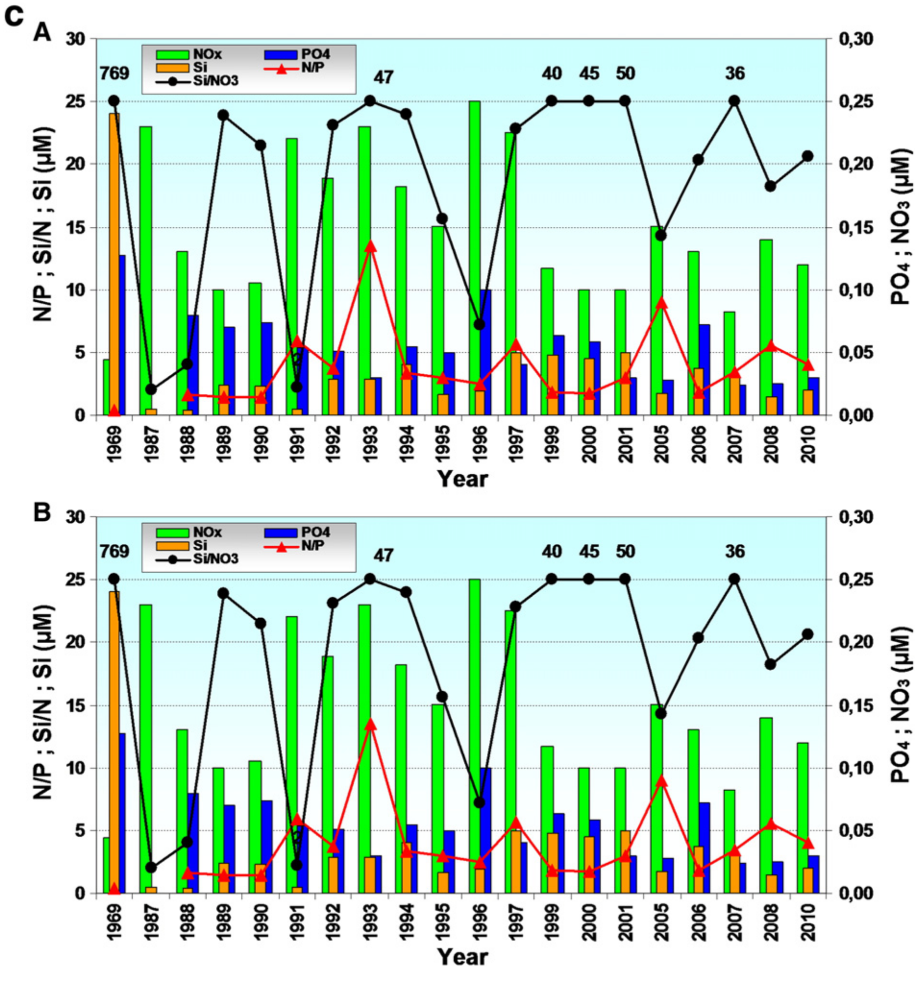

Fig. 4 (*continued*).

1998; Gregg and Yakushev, 2005; Oguz, 2002). In the region of the Rim Current, the chemocline onsets are depressed to smaller density surfaces by σ_t ~ 0.2–0.3 units (Fig. 3), but still occur at greater depths than in the central gyre because of strong current and formation of anticyclonic eddies (Codispoti et al., 1991; Ginsburg et al., 2002; Glazer et al., 2006; Oguz, 2002; Tugrul et al., 1992). The depth where O_2 decreases to suboxic concentrations (<20 µM) varies accordingly and ranges from $\sigma_t = 15.3$ to 15.6 during spring-summer period (Fig. 3) and agree nicely with the 2001 results of Konovalov et al. (2003). Similar distributions throughout the central Black Sea have been observed since the 1980s (Basturk et al., 1998; Çoban-Yıldız et al., 2006; Codispoti et al., 1991; Konovalov and Murray, 2001; Tugrul et al., 1992; Yakushev et al., 2009; Yiğiterhan et al., 2011). The strong halocline over the deep basin strongly limits vertical ventilation of O_2 to the SOL (Gregg and Yakushev, 2005; Oguz, 2002; Oguz et al., 2001) and O_2 becomes undetectable below the depth of $\sigma_t = 15.9$–16.0 in NW slope and central basin (Fig. 3). The SOL waters ($O_2 < 20$ µM) lie in the quasi-linear T–S regions, connecting the Bosporus outflow and CIL endmembers. Thus, waters of the SOL must originate from ventilation by the oxygenated Bosporus Plume (Konovalov et al., 2003) and the slope of the oxycline decreases in the SW Rim Current (Fig. 3).

The formation of a nitrate gradient zone (nitracline) in the oxycline is the result of aerobic respiration of POM in the upper halocline, reaching maximum concentrations just below the main oxycline at depths of $\sigma_t = 15.3$–15.5, where $O_2 \leq 20$ µM over the deep basin and rim current (Fig. 3). Its position has been stable over the last 3 decades (Çoban-Yıldız et al., 2006; Codispoti et al., 1991; Fuchsman et al., 2012; Tugrul et al., 1992; Yılmaz et al., 1998). However, when oxygen is depleted in the halocline the bacteria turn to nitrate as an electron acceptor (e.g., denitrification). Nitrate profiles in Figs. 2–3 from the west central gyre clearly show that the nitracline and oxycline were modified by the increased input of POM exceeding O_2 diffusion from the productive, well-oxygenated upper layer. This imbalance resulted in enlargement of the suboxic layer by ~15–20 m (σ_t ~ 0.2 units) and the onset of the nitracline shifted downward by σ_t ~ 0.3 units to the lower oxycline boundary and eroded the nitrate inventory of the central gyre in June 2001 (Fig. 3). Similar local changes in the vertical features were observed in July 1992 (Basturk et al., 1998). Moreover, this POM export to the halocline modified the distribution and isotopic composition of bulk POM in the oxycline and SOL of the central gyre (Çoban-Yıldız et al., 2006).

In the deep basin, dissolved oxygen and hydrogen sulfide do not co-exist at micromolar levels in the suboxic/anoxic interface where the nitrate also disappears (Figs. 2, 3). The first appearance of sulfide (>1 µM) has also been extremely stable at $\sigma_t = 16.15$–16.2 in the deep central basin though the sulfidic water boundary at nanomolar levels (<50 nM) has been observed to vary between the $\sigma_t = 16.0$–16.1 surfaces (Glazer et al., 2006), where phosphate profile displayed a steep increasing trend (Fig. 3).

The Rim Current in the SW shelf/slope region is also impacted by lateral intrusions of the oxygenated Bosporus Plume (Konovalov et al., 2003). This ventilation modifies the characteristic chemical structures in the suboxic/anoxic transition zone (Figs. 2, 3). The high resolution pump-cast profiles during Knorr 1988 and 2001 clearly show evidence of these injections with different hydro-chemical properties to intermediate depths of the western Rim Current and peripheries (Codispoti et al., 1991; Konovalov et al., 2003). The Bosporus Plume injects oxygen (200–250 μM) and nutrients (nitrate: 3–5 μM) into the SOL and upper anoxic (sulfidic) waters (Konovalov et al., 2003, 2005), leading to expansion of the bottom boundary of the SOL to greater depth and density surfaces. Konovalov et al. (2003) estimated that oxygen injected by the Bosporus Plume could oxidize a major fraction (>50%) of the sulfide produced annually by sulfate reduction in the interface. They concluded that the Bosporus Plume plays a crucial role for injecting oxygen into the upper sulfidic layer and for maintaining the first appearance of sulfide (>1 μM) at the depths of σ_t: 16.15–16.2 surface over the central basin. The large oxidation capacity (O_2, nitrate, oxidized Mn) of the Bosporus Plume was sufficient to oxidize sulfide in the anoxic interface and depress the first appearance of sulfide to deeper density surfaces (σ_t ~ 16.4–16.5) in the region of the SW shelf break (Konovalov et al., 2003). This ventilation also results in formation of secondary nitrate and nitrite maxima in the oxygen depleted (DO < 50 μM) transition zone as clearly shown in Figs. 2, 3, and also observed by Fuchsman et al. (2012) in 2001, 2003 and 2005. Oxygen, nitrate, ammonia, dissolved manganese and nitrite often co-exist in the SW Rim Current (Figs. 2, 3). The profiles of ammonia dissolved Mn (Fig. 3) and sulfide also display irregular distributions within the redox-gradient and sulfidic zone (Codispoti et al., 1991), due to the intrusions of Bosporus Plume. These modified vertical features decreased in intensity with increasing distance away from the Bosporus Plume in the SW Rim Current. The formation of a broad nitrite maximum in the mixing zone of Bosporus Plume also indicates the occurrence of intensive biomediated redox reactions such as autotrophic denitrification (Fuchsman et al., 2012), and aerobic/anaerobic oxidation of ammonium (Fuchsman et al., 2008; Kuypers et al., 2003) and oxidation/reduction of dissolved Mn (II, III) (Trouwborst et al., 2006; Yakushev et al., 2009).

O_2 profiles from the NW shelf/slope and central gyre were generally similar; but the main oxycline was steeper due to the thicker SOL formed in the central gyre (Fig. 3a). However, high-resolution pump cast profiles on the NW slope (Figs. 2, 3) demonstrate the existence of small irregular distributions in the upper nitracline, coinciding with changes in the slopes of the oxygen and silicate gradients. These features suggest that lateral intrusions from the shelf break into the rim current at the depth of the CIL may play a role. Modeling studies have simulated these ventilation fluxes and distributions from both the NW and SW shelf/slopes (Grégoire and Friedrich, 2004; Konovalov and Murray, 2001; Konovalov et al., 2005; Stanev and Beckers, 1999). The less dense, CIL waters from the NW shelf can only ventilate the main oxycline formed in the upper halocline, whereas the oxygenated, nitrate-rich, denser Bosporus Plume can intrude into the depths of SOL and the upper depths of the sulfidic layer down to depths of σ_t ~ 16.5 (Glazer et al., 2006; Konovalov and Murray, 2001; Konovalov et al., 2005; Ozsoy et al., 1993). Its effect can be traced even in the central basin (L2-St.13) where the nitrate displayed a secondary maximum at the σ_t ~ 16.0 depth and the Mn_d profile exhibited a coherent minimum (Fig. 8).

Intrusions of the Bosporus Plume also appear to enhance chemoautotrophic production (ChP) rates in the SW coastal region. Yılmaz et al. (2006) observed that ChP increased markedly in the sulfidic water interface, which coincided with the lower boundary of the fine particle layer in the region of Sakarya Canyon (downstream from the Bosporus outflow). Depth integrated ChP in this zone was actually greater than in the euphotic zone (Yılmaz et al., 2006). Though the effect of O_2 input from the Bosphorus plume on the sulfide budget of the subhalocline layer has been estimated (Konovalov and Murray, 2001), no detailed study has been carried out in the SW region to assess the quantitative role of the Bosporus Plume on the enhancement of POM production by ChP in the deepened redox gradient zone.

Phosphate profiles in Figs. 2, 3 clearly show a broad P-maximum located in the upper SOL, followed by an intense P-minimum persistently at the σ_t = 15.85–15.90 surfaces in the central gyre and its peripheries as previously reported (Codispoti et al., 1991; Murray et al., 1995; Tugrul et al., 1992). In this P-minimum zone, O_2 concentrations decreased to ≤5 μM levels, with no detectable vertical gradients in the central gyre. The depth of the P-minimum zone coincides with the increase in Mn_d and with the maximum in particulate Mn (Figs. 3, 7) (Yakushev et al., 2009; Yemenicioglu et al., 2006; Yigiterhan at al., 2011). The P-minimum is less intense in the SW Rim Current region and it almost disappears at some sites in the narrow coastal zone along the southern margin due to intensive mixing along similar isopycnal surfaces on the shelf break and slope (Basturk et al., 1998; Codispoti et al., 1991). The deep P-maximum, found just below the first appearance of sulfide (Codispoti et al., 1991; Sorokin, 2002; Tugrul et al., 1992), was located at the depths of σ_t = 16.15–16.20 in the NW slope and central gyre but at σ_t = 16.3–16.35 in the SW Rim Current (Fig. 3), due to intrusions of the oxygenated Bosporus Plume. Shaffer (1986) had proposed a Pumps-and-Shuttles model for these distributions that involved scavenging by iron (especially) and manganese oxides. More recent modeling of these complex reactions (Yakushev et al., 2007, 2009) suggest that particulate Mn oxides and dissolved Mn (III) play critical roles in formation of the features of the "phosphate dipole" in the redox gradient zone (O_2 < 5 μM and H_2S ~ 1.0 μM) over the deep basin. These features are due to P-adsorption on Mn oxides in the SOL, the formation of polyphosphate complexes with dissolved Mn (III) at the anoxic boundary and reduction of oxidized Mn to dissolved Mn (II) by sulfide ions (Luther et al., 1991), resulting in a steep increase and then formation of the deep P-maximum (Yakushev et al., 2009). In the SW Rim Current, intrusions of the Bosporus Plume into the redox gradient zone reduced the inventory of dissolved Mn in this zone by oxidizing Mn (II) to Mn (III) and Mn (IV) forms (Figs. 2, 3).

4.2. Spatial and temporal changes in surface water chemistry

Correlations between salinity and nutrient concentrations in the surface waters (0–10 m) of the NW shelf fed by riverine inputs and the Rim Current and surface distributions of nutrients in the western basin (Fig. 4a–b) show that the excess of riverine nutrients remained in the low salinity coastal waters (S < 16) off the Danube delta after consumption by autotrophic organisms. In March 1995, however, high riverine nutrient inputs influenced a larger area of the NW shelf (S < 17.5) compared to conditions in October 2005 (Fig. 4b). Spatial changes were more pronounced in the silicate and nitrate concentrations of NW shelf waters, decreasing from the less saline coastal waters to the shelf break and Rim Current due to uptake by algal organisms (Fig. 4a, b). In the Rim Current (S > 17.5), the surface nutrient concentrations (nitrate: 0.05–0.5 μM, Si: 2–10 μM, phosphate: 0.02–0.1 μM) did not show any trend with salinity, resulting in higher Si/N ratios (exceeding 100 in nitrate-depleted waters in summer as shown in Fig. 4a) but low N/P ratios (<10). In spring-summer, the surface layer of the western central gyre and its peripheries (S > 18) were depleted in nitrate (0.1–0.2 μM) and phosphate (0.02–0.05 μM), which were less than the coastal values (Fig. 4b, c). Surface silicate concentrations in the western basin were enhanced in winter (Si: 5–10 μM) due to input from the CIL depths by vertical mixing and then decreased apparently in April–October of 1988–2010 (Fig. 4b, c). However, surface nitrate and phosphate concentrations remained low in the deep basin in these periods due to limited inputs from the upper nutricline depths.

The Si/N ratios were relatively low (<10) in less saline coastal waters (S < 16), due to the low silicate content (compared to nitrate concentrations) of rivers discharging to the NW shelf (Oguz et al., 2008). The surface Si/N ratios increased by 5–10 fold from the inner shelf to offshore waters of the NW shelf (S ~ 16.5–17.5) (Fig. 4b). The Si/N ratios markedly increased in the Rim Current (S > 17.5) and central gyre because Si concentrations increased from the coastal region to the central basin while the nitrate concentrations remained low (Fig. 4a–c).

In October, the N/P ratios in the nearshore waters off the Danube delta were much higher (>20), decreasing below 10 with increasing salinity in the inner shelf waters (S < 16) while the Si/N ratios remained very low (<2) (Fig. 4a). This was a low flow period of the Danube in October 2005 when nitrate inputs were much greater than the phosphate in the brackish surface waters (S < 15) (Fig. 4a, b). However, this ratio was markedly low in the less saline, nutrient-depleted waters of the inner shelf off the Dnieper delta (Fig. 1) visited in June 2001 (Fig. 4a). The N/P ratios generally decreased below 10 in the nitrate and phosphate-depleted surface waters of the coastal margin and the Rim Current (S = 17.5–18) in April–October (Fig. 4a). However, in late March 1995, the N/P ratios were high (>10) in the nitrate-excess waters of the Rim Current. In winter, the N/P ratio increased in the NW shelf and SW coastal region due to excess nitrate inputs from both the major rivers and the nitrate-laden CIL by intensive vertical mixing (Cociasu et al., 1996) and decreased uptake of nutrients by phytoplankton.

Before the 1960s, in the period before damming of the major rivers and preanthropogenic Black Sea, unpolluted major river discharges fed the NW shelf with high concentrations of silicate and nitrate but low phosphate concentrations (Ludwig et al., 2010). Therefore, the river inputs had very high N/P but low Si/N ratios until the mid 1970s (Cociasu et al., 1996; Oguz et al., 2008). After construction of big dams on the major rivers (mainly the Danube) by the early 1970s, the silicate content of the river water decreased markedly and the rivers became increasingly polluted by dissolved inorganic nitrogen (DIN: nitrate + ammonium) and phosphorus discharges from agricultural, industrial and domestic sources. The nutrient loads of the Danube River gradually decreased after the mid 1990s, but the N/P ratio stayed high (>25) (Oguz et al., 2008; Strokal and Kroeze, 2013).

Comparison of 1960s and more recent data sets (1987–2010) from the SW coastal and west central gyre (Fig. 4c) indicate sharp decreases in the silicate content of the surface layer (0–10 m) after the mid 1970s as compared to the winter and summer concentrations of the 1988–2010 period. The surface silicate concentrations declined drastically to levels of 0.1–0.5 μM in the SW coastal waters in late summer–early fall of 1988, 1991 and 2005, and even in the central gyre (S > 18) in July 1988. This change reduced the Si/N ratio dramatically from values as high as 700–900 to very low levels (<1.0) in the western coastal regions in some years after the 1970s (Fig. 4), especially the most eutrophic period between 1987 and 1991 when DIN (mainly in the form of nitrate) and phosphorus inputs by the Danube were at the highest levels (Oguz et al., 2008). In the last two decades, significant decreases in the Si/N ratio in the DIN-enriched river waters (mainly the Danube) with low phosphate concentrations plus possible increases in DIN inputs by low Si wet deposition (Medinets and Medinets, 2012) have led to consumption of excess silicate and phosphate in the shelf and open surface waters (Humborg et al., 1997; Konovalov and Murray, 2001). The surface silicate concentrations of the central gyres increased gradually to 5–7 μM in the early 1990s (Fig. 4c) and have remained higher than in the coastal waters. In this period nutrient (DIN and TP) discharges to the major rivers were reduced (Oguz et al., 2008) and silicate supply from the halocline depths (reaching up to 10 μM in late March by winter mixing) became sufficient for consumption (Fig. 4c). In the central gyre, the annual averages of the Si/N ratios for the surface mixed layer (0–10 m) have mostly remained high (>25), even exceeding 100 in nitrate-depleted regions and after winter mixing (Fig. 4a, c).

In the 1950ss–1960s, waters discharged from the Danube, other major rivers and wet precipitation entered the Black Sea with high values of nitrate/phosphate (N/P) molar ratios (>50) due to high inputs of anthropogenic DIN but with low anthropogenic inputs of phosphate (Ludwig et al., 2010; Oguz et al., 2008). However, in the 1960s, the N/P ratio was very low (<1–5) in the oxygenated upper layer waters (Fig. 5) due to the unexpectedly low nitrate concentrations compared to phosphate. Therefore, unexpected long-term trends were seen in the nitrate and phosphate concentrations and their molar (N/P) ratios in the less saline surface waters of the western central gyre and SW coastal waters (Figs. 4–5). The major change occurred for phosphate, which was as high as 0.1–0.3 μM before 1970 (Fig. 4c) when algal production was low and the euphotic zone thickness of 40–50 m extended down to the upper nutricline in the central basin. Though the nitrate-laden major rivers were relatively poor in phosphate, the Black Sea surface waters were relatively rich in phosphate during this early pre-dammed or “pristine” period. Then, after the 1970s, surface phosphate concentrations in the central basin decreased to nearly undetectable levels of 0.02–0.05 μM, due to large inputs of anthropogenic DIN (mainly as nitrate) with high N/P ratios, leading to consumption of excess phosphate and silicate in the surface waters over the basin (Fig. 4c). Surface nitrate concentrations of the Rim Current and central gyre were very low (0.02–0.1 μM) before the 1970s though the major rivers carried nutrients to the sea with high N/P ratios (Ludwig et al., 2010; Oguz et al., 2008). After the mid 1970s, nitrate concentrations in the surface layer increased significantly, exceeding 5.0 μM in the NW coastal waters (S < 17.5) (Cociasu et al., 1996) and 0.2–0.3 μM in the central gyre during winter-early spring period (Fig. 4a–b). After the mid 1990s, the surface nitrate and phosphate concentrations have decreased gradually in the central gyre (Fig. 4c).

High values of the N/P ratio in the NW coastal waters (S < 16) fed by the Danube inputs strongly suggest P-limited algal production (Oguz et al., 2008). However, the low N/P ratios (<10) in surface waters of the Rim Current and central gyre (in Fig. 4c) and previous bioassay results (Yayla et al., 2001) indicated that nitrate was the potential limiting

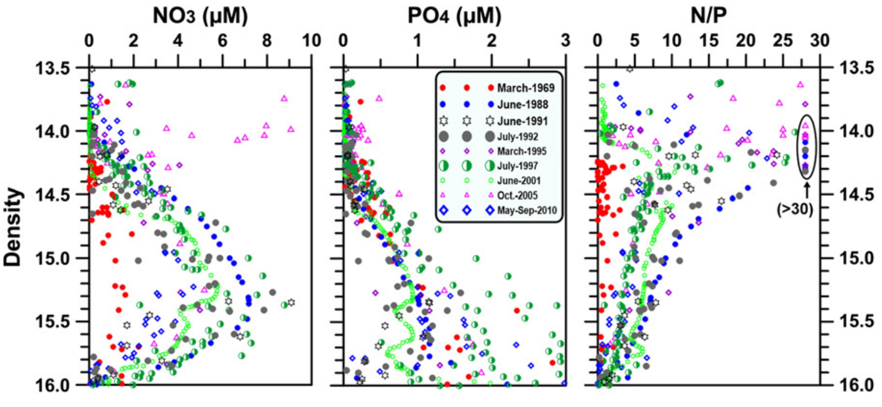

Fig. 5. Representative profiles versus density of nitrate, phosphate and their molar (N/P) ratios in oxic/suboxic layers of the SW coastal margin in 1969, and between 1988 and 2010.

nutrient for algal production in the central basin during spring-autumn period. The low Si/N ratios observed seasonally in the Rim Current and shelf waters and occasionally in the central gyre implied that there is also potential Si limitation on primary production.

4.3. Temporal changes in the water column chemistry

The riverine silicate input to the surface layer declined after the mid 1970s as the increased input of nitrate (>600 kton y^{-1}) and phosphate (~40 kton y^{-1}) in the 1980s was enhancing eutrophication in the NW shelf and western basin (Cociasu et al., 1996; Oguz et al., 2008). The enhanced POM production and sedimentation to the halocline depths drastically changed the nutrient inventories of the NW shelf (Cociasu et al., 1996; Humborg et al., 1997), where the source waters of the CIL form during winter cooling and mixing (Tolmazin, 1985). The limited historical data depicted in Fig. 5 from the SW coastal region suggest that in late March 1969, the surface and upper CIL waters ($\sigma_t < 14.5$) of SW Rim current were relatively poor in nitrate, increasing slightly from <0.05 μM in the surface to 0.1–0.2 μM in the upper CIL, where the phosphate ranged from 0.06 to 0.2 μM (Brewer, 1971). Estimates of the N/P ratio at that time were unexpectedly very low (<2) in the oxygenated CIL and the oxycline between $\sigma_t = 14.5$–15.6 (Fig. 5). In June 1988, the upper CIL of the SW shelf zone (between 30 and 60 m depths where σ_t: 14.0–14.3 and salinity: 18.15–18.3) were still very poor in phosphate (0.02–0.07 μM) but became more enriched in nitrate (Codispoti et al., 1991), increasing from 0.1–0.15 μM at 20–30 m to 2.0–3.0 μM between 40 and 60 m (where σ_t: 14.2–14.4, Fig. 5) in the upper CIL, leading to very high N/P ratios (>50). However, warmer winter conditions in 2001 limited the formation of CIL (core temp. > 7.0 °C in June) and resulted in less export of nutrients from the NW shelf to the intermediate depths of the western basin (Oguz and Ediger, 2006; Oguz et al., 2006). This led to changes in the biochemical properties of the euphotic zone (1% light depth) (Oguz and Ediger, 2006; Yılmaz et al., 2006) and also in the transition zone properties in the west central basin as discussed above and previously (Çoban-Yıldız et al., 2006). The nutrient content of the CIL in the western Rim Current varies inter-annually (Fig. 5), depending on in the nutrient fluxes by the major rivers and temperature changes in the CIL waters (Glazer et al., 2006; Gregg and Yakushev, 2005; Oguz, 2008). Variable nitrate concentrations in the upper CIL remained high during the cooler period of 1987–1991 (Oguz et al., 2008) whereas the phosphate was less than 0.1 μM, resulting in significant increases in the N/P ratio which reached maximum values (>30) between the depths of σ_t: 13.9–14.4 surfaces (Fig. 5). The silicate and phosphate inventories of the CIL decreased from the 1960s to the 1980s (Cociasu et al., 1996). The CIL waters with temporally variable properties flow towards the southwestern region and central gyres. They have been observed to flow into the Sea of Marmara, with very high nitrate (>5.0 μM) and high N/P ratios during December–February period of the 1990s (Polat and Tugrul, 1995). This increasing nutrient input from the Black Sea has enhanced not only eutrophication in the Marmara Sea but also the nitrate and phosphate inventories of the suboxic deeper layer since the 1970s (Polat et al., 1998).

The long-term decline in the surface silicate concentrations has become pronounced (Fig. 4c), with maximum concentrations decreasing from 50 to 70 μM levels in the 1950s to <1.0 μM in late 1980s (Codispoti et al., 1991). This change indicates a decline of about 1500 mmol m^{-2} in the Si inventory of the less saline surface layer (0–30 m) over 25–30 years. After reduction in the riverine nitrate and phosphate inputs after the mid-1990s (Oğuz et al., 2008), the Si inventory in the surface layer of the deep basin increased gradually, varying regionally and annually between 50 and 200 mmol m^{-2}, depending on inputs from the major rivers and the upper halocline depths. The surface silicate concentrations still remained below 10 μM in the Rim Current and central basin in the late winter (Fig. 4a–b) and then decreased locally to 1–5 μM during the spring–autumn period (Fig. 4c).

We used the corrected silicate data of the Atlantis 1969 survey (Brewer, 1971) to estimate temporal changes in Si inventories of the deep basin. Si profiles in Fig. 6 from different years show drastic decreases in Si inventories of the upper layer after the 1970s. The integrated Si inventory from the surface to 150 m (σ_t ~ 16.4–16.5) was estimated to range between 9,100 and 10,600 mmol m^{-2} in the central basin in March 1969 and decreased to 6,000–7,000 mmol m^{-2} in the rim current. These inventories were probably 10% less than the inventories before the 1960s when the surface waters contained 50–70 μM silicate (Sorokin, 2002). The Si inventory of the upper 150 m in the 1960s was probably 25% greater than those in the summer of 1988, ranging regionally from 3,600 to 8,300 mmol m^{-2} in 1988, with an average value of about 7,500 mmol m^{-2} for the central basin. The Si inventory of the upper layer decreased slightly to levels of 7,000–7,500 mmol m^{-2} in the central basin from 1991 to 2005. Assuming a decrease of nearly 2,500 mmol m^{-2} in the Si inventory of the upper 150 m from the 1970s to early 1990s, the total amount of Si exported to the sulfidic layer below 150 m is estimated to be ~2.5×10^7 tons, equivalent to about 20-year Si input from the Danube from 1970 to 1988 (Konovalov and Murray, 2001). This suggests that the Si fluxes have approached steady state since the mid 1990s when the inputs of anthropogenic N, P to the Danube were reduced and the offshore silicate values have increased slightly (Figs. 4–5).

Increases in the nitrate inventory of the central basin after the 1960s have been documented by different groups (Codispoti et al., 1991; Konovalov and Murray, 2001; Tugrul et al., 1992). These changes are due to increased nitrate loads of the major rivers with modified Si/N/P ratios (Cociasu et al., 1996; Oguz et al., 2008). No decadal changes have been observed in the phosphate inventory of the upper layer from the surface to the P-minimum zone (Fig. 6) though the inventory of nitrate has increased by about 2–4 times under the increased stresses of denitrification in the enlarged SOL (Konovalov and Murray, 2001) and then decreased gradually after the mid-1990s. However, the nitrate inventories of the central gyre were subject to considerable interannual variability in spring-summer period, reaching the maximum levels of 250–280 mmol m^{-2} in the late 1980–early 1990s when the riverine nutrient inputs were at maximum levels (Baştürk et al., 1998; Konovalov and Murray, 2001; Oguz et al., 2008). They then decreased to levels of 150–200 mmol m^{-2} in the more recent decades, even further to ~100–120 mmol m^{-2} in the west central gyre in July 1992

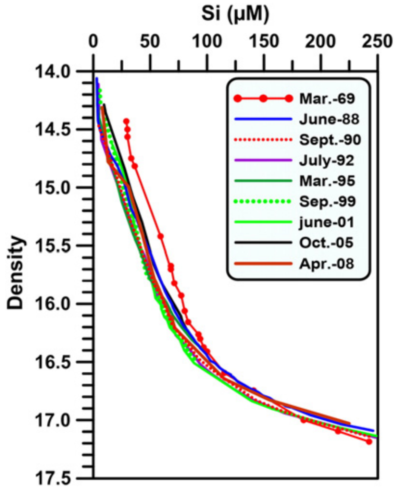

Fig. 6. Vertical distributions versus density of silicate in the western central gyre (historical data are from the Atlantis-1969, Knorr-1988, 2001, Parshin-2005 and Bilim multicruises in the western Black Sea).

(Baştürk et al., 1998) and in June 2001 (Figs. 2–3). Such drastic nitrate loss in the nitracline occurred when the upper nitracline was eroded by increased denitrification at the upper boundary of the SOL enlarged locally by greater POM sinking from the surface layer than the O_2 diffusion into the oxic/suboxic interface in the CIL (Çoban-Yıldız et al., 2006; Oguz and Ediger, 2006).

Density-dependent chemical profiles in Figs. 3, 7 provide insight to regional variations in the chemical properties of the oxic/anoxic transition zone of the coastal, shelf break and central basin. The oxycline, commencing at depths of σ_t: 14.2–14.5, vanishes at the nitrate maximum zone found at σ_t:15.3–15.5 in the northern and central basin, but deepens in the SW coastal margin. The phosphate minimum is found between σ_t: 15.85–15.90 where $O_2 \leq 5.0$ μM and dissolved Mn commences to increase, followed by the increase in ammonia at the depth of σ_t ~ 16.0, the increase in reduced iron at σ_t ~ 16.05–16.1 and the first appearance of sulfide (>1.0 μM) at σ_t ~ 16.15–16.2 as predicted from their redox potentials. The density surfaces of these distinct features have remained almost unchanged in the west central gyre since the 1980s (Konovalov and Murray, 2001; Konovalov et al., 2003; Murray et al., 1989, 1995; Tugrul et al., 1992; Yakushev et al., 2009). However, the boundaries and gradients of chemical features in permanent halocline show considerable regional variability as discussed in Section 4.1 (Figs. 2–3), especially in the WS Rim Current and anticyclonic eddies (Basturk et al., 1998; Codispoti et al., 1991; Oguz, 2002).

The suboxic and anoxic, sulfidic waters in the SW coastal region and Rim Current are impacted by lateral intrusions of the oxygenated (200–250 μM) Bosporus Plume as emphasized previously (Codispoti et al., 1991; Konovalov et al., 2003). This oxygen supply was estimated to oxidize the majority (>50%) of sulfide produced in the upper sulfidic layer by anaerobic bacteria (Konovalov and Murray, 2001) and observed to reduce sulfide concentrations slightly in these waters (Codispoti et al., 1991). However, after the 1970s, the Bosphorus Plume has been injecting less oxygen (by at least 20–30%) but more nutrients (Fig. 5) into the intermediate depths of the SW Black Sea due to decreases in both the oxygen concentrations of CIL waters (Figs. 3, 8) and Bosphorus underflow (Polat and Tugrul, 1995) by 100–150 μM. Eutrophication development in both seas has reduced the thickness of the euphotic zone (Polat et al., 1998; Oguz et al., 2008), resulting in more POM export below the photic zone and more O_2 consumption and nitrate accumulations in the CIL (Figs. 3, 5) and Marmara lower layer (nitrate ~ 8–10 μM, O_2 ~ 30–50 μM).

Close examination of the vertical features of the redox sensitive Mn (dissolved, particulate), phosphate (by combining P adsorbed by Mn oxides and dissolved species), nitrate and oxygen in Figs. 7–8, strongly suggest a long-term upward shift in the depth of P-minimum zone and the onset of dissolved Mn to $\sigma_{t:}$~15.85–15.90. In the 1960s, the P-minimum was less pronounced and located at greater (deeper) density surfaces (between $\sigma_{t:}$: 16.10–16.15) (Fig. 7); it was barely detectable in the oldest studies (Sorokin, 2002; Tugrul et al., 1992), presumably due to the coarse sampling of the redox gradient zone that was much thinner (about 10 m thick) at that time (Fig. 7). The deep phosphate minimum consistently coincided with the Mn_d onset at the depth where $O_2 \leq 5$ μM (Figs. 7–8). The upward expansion of the O_2-depleted zone (≤5 μM) by ~0.15 density units (~15–20 m) has probably shifted the position of the Mn_p maximum and the onset of increasing Mn_d and Fe^{2+} (Figs. 3, 7) upward compared to their position in the late 1960s (Spencer and Brewer, 1971; Spencer et al., 1972). The deep P-minimum and Mn_d onset at the $O_2 \leq 5.0$ μM boundary have been formed consistently at σ_t ~ 15.85–15.90 (Figs. 3, 7) as reported by Trouwborst et al. (2006), Yemenicioglu et al. (2006) and Yakushev et al. (2007, 2009) even though microbial oxidation of Mn (II) at sub-micromolar O_2 concentrations were observed to occur in the suboxic/anoxic interface (Clement et al., 2009). These findings support apparent changes in the gradient of the Mn_d profiles shown in Fig. 3 from the SW Rim Current impacted by the Bosporus Plume and decreases in Mn_d/P ratios in the suboxic/anoxic interface as compared to those in the central basin (Fig. 7). Trouwborst et al. (2006) and Yakushev et al. (2009) also suggested that dissolved Mn (III), which was at nearly undetectable concentrations at the upper boundary of the P-minimum zone, where the Mn_d/P ratios displayed a coherent maximum (Fig. 7), has a key role on the formation of "phosphate dipole" in the suboxic/anoxic boundary zone by combining with polyphosphate ions and reduction by sulfide ions in the anoxic interface. The oxidation of Mn (II, III) at sub-micromolar levels of O_2 (Clement et al., 2009) can explain how the particulate Mn maximum was formed within the suboxic/anoxic interface before the 70s (Spencer and Brewer, 1971; Spencer et al., 1972) and its upper shift by ~0.2 σ_t units to the $O_2 \leq 5$ μM boundary situated at σ_t = 15.85–15.9 surfaces in recent decades (Trouwborst et al., 2006; Yakushev et al., 2009; Yigiterhan et al., 2011).

The coincidence of the deep phosphate maximum with the first appearance of sulfide is probably the result of dissolution of phosphate-associated Mn (III) complexes with sulfide (Kostka et al., 1995; Trouwborst et al., 2006 and Yakushev et al., 2007, 2009) whereas the maximum of Mn_p, which disappears above the sulfidic boundary, possibly contributes to the formation of the steep phosphate gradient in the anoxic interface (Codispoti et al., 1991; Murray et al., 1995). Thus, the "phosphate dipole" (minimum, steep gradient and maximum) can be used as a supplementary parameter to assess long-term changes in

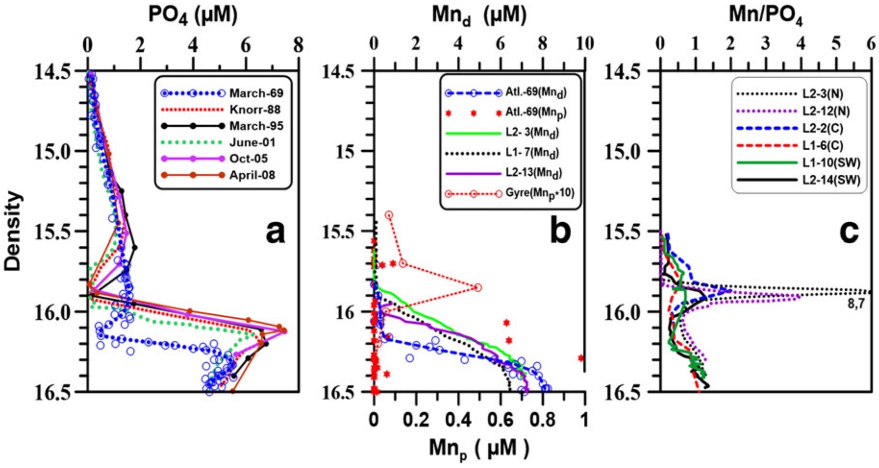

Fig. 7. Vertical distributions versus density of (a): phosphate (PO_4) from different years, ((b): dissolved and particulate manganese (Mn_d, Mn_p) (historical manganese data from the 1969 Atlantis data of Spencer and Brewer (1971) and Spencer et al. (1972) and the new manganese data from the May–June 2001 Knorr cruise [Mn_p data from the Yigiterhan et al. (2011)]), and (c): Mn_d/PO_4 ratio in the upper layer of the western central gyre of the Black Sea in May–June 2001.

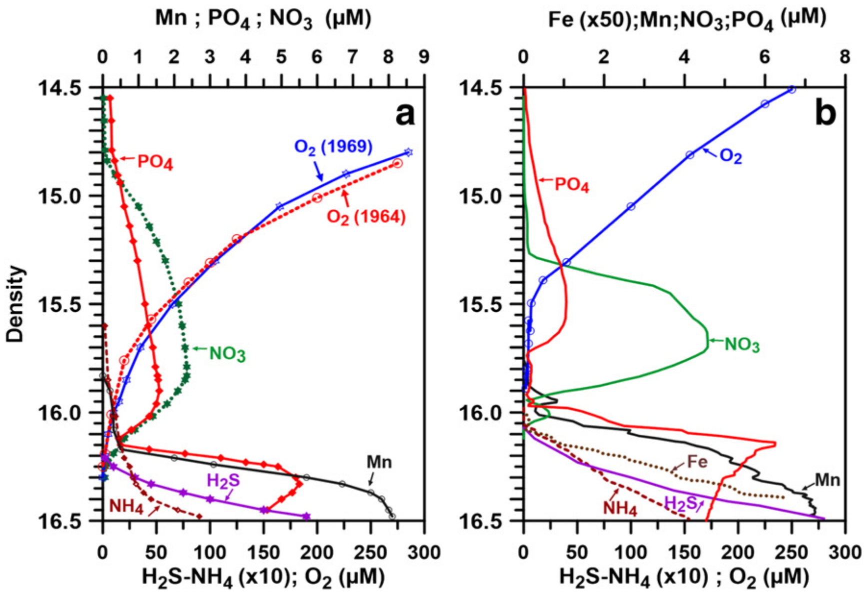

Fig. 8. Vertical distributions versus density of dissolved oxygen, hydrogen sulfide, phosphate, nitrate, nitrite, dissolved manganese and reduced iron in the oxic, suboxic and upper anoxic layers of the western central gyre of the Black Sea: (a, left panel): In March 1969 (old data from Brewer (1971), Spencer and Brewer (1971), and Spencer et al. (1972); best-fit old profiles of Mn and P from Fig. 7 and the summer oxygen profile from 1964); (b): In early June 2001 (data obtained during the June 2001-Knorr cruise).

the boundaries of the redox gradient ($O_2 \leq 5.0$ µM) and the anoxic sulfidic layer in the deep basin. The upward shift of both the depths of particulate Mn maximum and dissolved Mn (III) onset by the enlarged SOL in the deep basin probably have reduced upward diffusion of phosphate from the P-maximum zone at the anoxic boundary (σ_t ~ 16.2) after the 1970s. However, in the SW Rim Current, where the redox gradient zone is relatively thin (5–10 m) and located at greater depths and density surfaces (Fig. 3), and Mn_p-rich "fine particle layer" has been situated within the P-maximum zone below σ_t ~ 16.1 depths. Therefore, the southern Rim Current regions are more favorable for phosphate diffusion from the P-maximum boundary to the upper nutricline, which is likely to be similar to the "pristine" conditions seen over the basin.

The apparent upper shift of the oxidizing agents (O_2, nitrate and Mn) of ammonium ions after the 1970s, is very likely to have led to similar long-term changes in the onset of increasing ammonium and their gradients in the suboxic/sulfidic layer interface in the deep basin (Fig. 8) as suggested by Konovalov and Murray (2001). Dissolved Mn (III) may also oxidize ammonium ions diffusing into the redox gradient zone from the sulfidic layer over the basin (Trouwborst et al., 2006; Yakushev et al., 2009) and a (nitrate + ammonia)-N deficient zone with a thickness of about 5–15 m has been formed in this layer, enlarging in the central gyre (Fig. 8).

Though rivers and wet precipitation have supplied nutrients to the Black Sea with high N/P ratios (Ludwig et al., 2010), the surface waters over the basin had excess phosphate (0.1–0.3 µM) but very low nitrate concentrations in the pre-anthropogenic "pristine" period, resulting in very low N/P molar ratios (Fig. 4). Similar low N/P ratios (<2.0) derived from regression analysis of data from the nutricline to the nitrate maximum zone, have been observed in the main oxycline vanishing at the nitrate maximum depths. The N/P ratio for the 1960s was much smaller than the classical Redfield N/P ratio of 16 in the oxygenated deep oceans and in the ratio (~10) in the O_2-depleted but nutrient-enriched, higher salinity, lower layer waters of the Marmara Sea fed by the Black Sea outflow (Polat et al., 1998). The Apparent Oxygen Utilization/Phosphate, AOU/Nitrate and nitrate/phosphate (N/P) ratios were obtained from regression analyses of the March1969, March–April 1995 and 1988–2008 data sets obtained in the main oxycline down to the nitrate maximum depth over the deep basin (Fig. 9). The AOU/P ratio has remained high (160–230) since the late 1960s (Fig. 9), which are comparable with ratios (~180) in the suboxic lower layer of Marmara Sea (Polat et al., 1998). However, in March 1969, the AOU/N was very high (125) and was much greater than the ratios of ~40 for 1988–2008 period, and

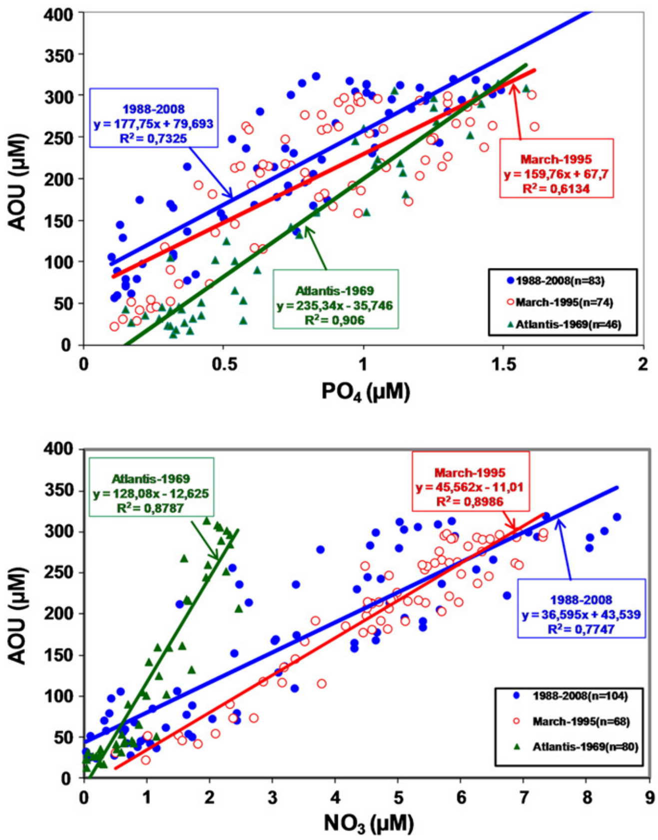

Fig. 9. Variations of nitrate (N) and phosphate (P) concentrations relative to apparent oxygen utilization (AOU) in the oxycline and upper SOL boundary down to the depth of the nitrate maximum in March 1969, late March–April 1995 and 1988–2008 periods.

the ratios of ~ 20 in the Marmara lower layer and the classic Redfield ratio of ~9. Very low N/P (<2) and markedly high AOU/N ratios in the nitracline of the deep basin before the 1970s strongly suggest that nitrate removal by POM oxidation (denitrification) was highly effective within oxic/suboxic interface of 5–10 m thick, located between the depths of $\sigma_t = 15.0–5–15.4$ in recent decades, where $O_2 < 75$ μM, resulting in apparent imbalance between AOU and the nitrate increases. The nitrate was still very low at the base of the main oxycline (Fig. 8) where $O_2 < 75$ μM (or AOU > 200 μM) and the phosphate increased steadily. Increased POM export below the photic zone enhanced O_2 removal by microbial oxidation-reduction processes and decreased the steep oxycline thickness further and enlarged SOL upward in June 2001 as nitrate removal was fueled by POM oxidation at the suboxic boundary in the western central gyre in the summer of 1992 and 2001 (see Fig. 8). Moreover, denitrification, anammox and oxidation/reduction processes below the nitrate maximum zone down to the sulfidic water boundary (from σ_t:15.6 to 16.1) enhance nitrate removal to molecular nitrogen ($N_{2)}$ in the O_2-depleted layer (Glazer et al., 2006; Koeve and Kahler, 2010; Murray et al., 1995). The formation of the chemocline with very low N/P ratios (<2) but very high AOU/N ratio (~125) in the Black Sea oxic/anoxic transition zone in the 1960s has been poorly understood. It is yet unresolved what processes created drastic imbalance between AOU and nitrate increases in the oxycline/SOL interface.

5. Conclusions

There have been long-term changes in the inputs of nutrients to the Black Sea. The main changes have been an increase in DIN input due to increased anthropogenic sources and a reduction in silicate input due to construction of big dams. These changes have altered the distributions and inventories of nutrients in the surface and suboxic layers of the Black Sea.

Before “pre-damming of the major rivers” in the 1960s, the major rivers with high nitrate and silicate concentrations fed the Black Sea which contained excess amounts of silicate and phosphate but very low nitrate concentrations (resulting in very high Si/N but very low N/P ratios) The terrestrial (river + precipitation) inputs of DIN were not sufficient for consumption of the excess inventories of Si and P in the surface waters of the coastal and central gyres until the late 1960s. This suggests that P-uptake in the surface layer was compensated by input from the oxycline having a feed-back from the P-maximum zone in the sulfidic interface. After the mid 1970s, increased DIN and phosphate but reduced Si inputs by the major rivers, which had low Si/N but high N/P ratios, enhanced eutrophication over basin and POM export to the halocline depths. This change resulted in significant decreases in the Si and phosphate inventories and the Si/N ratio but marked increases in the N/P ratio in the low salinity surface layer (0–30 m), the upper CIL and the main oxycline (Fig. 5). The AOU-nitrate-phosphate correlations in the main oxycline of the Black Sea (yielding very low N/P but very high AOU/N ratios) are much different from those in the suboxic waters of the Marmara Sea which is fed by the Black Sea outflow whereas the AOU/P ratios are similar. The increased POM export from the surface layer has enlarged the SOL in the central gyre. This triggered changes in the redox-dependent properties of the suboxic/anoxic interface in the deep basin. The depths of the major chemical features (the depths of P-minimum, Mn_p maximum and Mn_d onset) have shoaled by 10–20 m, by following the depth of the DO ≤ 5 μM boundary. Most importantly, the enlarged SOL may have increased the role of dissolved Mn (II, III) and particulate Mn oxides on the formation of the “P-dipole feature” formed between σ_t: 15.85–16.2 surfaces in the suboxic/sulfidic water interface. The oxidation and complex formation capacity of Mn (III) possibly limited upward transport of ammonium and phosphate from the anoxic boundary into the upper SOL of the central gyre where the profiles of nitrate, ammonium and phosphate display intense minima in the lower suboxic zone ($O_2 < 5$ μM), reflecting strong sinks of these nutrients at those depths (Fig. 2–3). The upward flux of phosphate from the P-maximum zone is expected to be greater in the shelf/slope region where the P-minimum zone weakens apparently (Fig. 2–3), the redox gradient zone ($O_2 < 5$ μM) is below the P-maximum and much thinner (~10 m), and the Mn_p maximum is formed within the broad “fine particulate layer” situated between the depths of σ_t:16.1–16.4 density surfaces (Yiğiterhan et al., 2011). The SOL of the SW coastal region fed by O_2 and nitrate-rich Bosphorus Plume needs to be further studied to better understand aerobic/anaerobic oxidation processes of dissolved Mn(II, III) and ammonia, the nitrate removal by denitrification and POM synthesis by chemoautotrophic production in the redox gradient zone.

Acknowledgments

We are grateful to the technicians Saim Cebe and Esabil Kakaç from METU — Institute of Marine Sciences for nutrient and dissolved oxygen-hydrogen sulfide measurements and help in the figures. The authors also thank two anonymous reviewers for their helpful comments and suggestions. We also thank the crew and captains of R/V BILIM, KNORR and PARSHIN for their help during the field surveys. This work was partly supported by the NATO-SfP, GEF-BS, EU-FP6 (SESAME Project, Grant #: 036949) and EU-FP7 Programs (PERSEUS Project, Grant #: 287600), and TUBITAK (SINHA, Grant #: 107G066 and others). Additional funding came from NSF Grant OCE 0649223.

References

Basturk, Ö., Tugrul, S., Konovalov, S., Salihoğlu, İ., 1998. Effects of circulation on the spatial distributions of principle chemical properties and unexpected short- and long-term changes in the Black Sea. In: Ivanov, L.I., Oğuz, T. (Eds.), Ecosystem Modeling as a Management Tool for the Black Sea. NATO Science Series, vol. 47. Kluwer Academic publishers, Netherlands, pp. 39–54.

Berlinski, N., Garkavaia, G., Bogatova, Y., 2003. Problems of anthropogenic eutrophication and evolution of hypoxic situations in the North-Western part of the Black Sea. Ecol. Sea 17–22.

Brewer, P.G., 1971. Woods Hole Oceanographic Institution, Unpublished Technical Report, Ref. No. 71-65 (92 pp).

Brewer, P.G., Murray, J.W., 1973. Carbon, nitrogen and phosphorus in the Black Sea. Deep-Sea Res. 20 (9), 803–818.

Clemet, B.G., Luther III, G.W., Tebo, B.M., 2009. Rapid, oxygen-dependent microbial Mn (II) oxidation kinetics at sub-micromolar oxygen concentrations in the Black Sea suboxic zone. Geochim. Cosmochim. Acta 73, 1878–1889.

Çoban-Yıldız, Y., Altabet, M., Yılmaz, A., Tuğrul, S., 2006. Carbon and nitrogen isotopic ratios of suspended particulate organic matter (SPOM) in the Black Sea water column. Deep-Sea Res. II 53, 1875–1892.

Cociasu, A., Dorogan, L., Humborg, C., Popa, L., 1996. Long-term ecological changes in Romanian coastal waters of the Black Sea. Mar. Pollut. Bull. 32, 32–38.

Codispoti, L.A., Friederich, G.E., Murray, J.W., Samatamota, C.M., 1991. Chemical variability in the Black Sea: implications of data obtained with a continuous vertical profiling system that penetrated the oxic/anoxic interface. Deep-Sea Res. 38 (Suppl. 2), 691–710.

Fuchsman, C.A., Murray, J.W., Konovalov, S.K., 2008. Concentration and natural stable isotope profiles of nitrogen species in the Black Sea. Mar. Chem. 111, 90–105.

Fuchsman, C.A., Murray, J.M., Staley, J.W., 2012. Stimulation of autotrophic denitrification by intrusions of the Bosporus Plume into the anoxic Black Sea. Front. Microbiol. 3, 257. http://dx.doi.org/10.3389/fmicb.2012.00257.

Ginsburg, A.I., Kostianoy, A.G., Nezlin, N.P., Soloviev, D.M., Stanichny, S.V., 2002. Anticyclonic eddies in the northwestern Black Sea. J. Mar. Syst. 32, 91–106.

Glazer, B.T., Luther III, G.W., Konovalov, S.K., Friederich, G.E., Trouwborst, R.E., Romanov, A.S., 2006. Documenting the spatial and temporal variability of the Black Sea suboxic. zone with in situ voltammetry. Deep-Sea Res. II 53, 1756–1768.

Grasshoff, K., Erhardt, M., Kremling, K., 1983. Methods of Sea Water Analysis, 2nd ed. Verlag Chemie GmbH (419 pp.).

Gregg, M.C., Yakushev, E., 2005. Surface ventilation of the Black Sea's cold intermediate layer in the middle of the western gyre. Geophys. Rec. Lett. 32, L03064.

Grégoire, M., Friedrich, J., 2004. Nitrogen budget of the northwestern Black Sea shelf inferred from modeling studies and *in situ* benthic measurements. Mar. Ecol. Prog. Ser. 270, 15–39.

Humborg, C., Ittekot, V., Cociasu, A., v. Bodungen, B., 1997. Effect of Danube River dam on Black Sea biogeochemistry and ecosystem structure. Nature 386, 385–388.

Karl, D.M., Knauer, G.A., 1991. Microbial production and particle flux in the upper 350 m of the Black Sea. Deep-Sea Res. 38, 921–942 (Suppl.).

Kıdeyş, A.E., 2002. Decline and recovery of a large marine ecosystem, the Black Sea. Science 297, 1482–1484.

Koeve, W., Kahler, P., 2010. Heterotrophic denitrification vs. autotrophic anammox-quantifying collateral effects on the oceanic carbon cycle. Manuscript prepared for, Biogeosciences 2327–23337.

Konovalov, S.K., Murray, J.W., 2001. Variations in the chemistry of the Black Sea on a time scale of decades (1960–1995). J. Mar. Syst. 31, 217–243.

Konovalov, S.K., Luther, G.W., Friedrich, G.E., Nuzzio, D.B., Tebo, B.M., Murray, J.W., Oğuz, T., Glazer, B., Trouwborst, R.E., Clement, B., Murray, K.J., Romanov, A.S., 2003. Lateral injection of oxygen with the Bosphorus plume-fingers of oxidizing potential in the Black Sea. Limnol. Oceanogr. 48 (6), 2369–2376.

Konovalov, S., Murray, J.W., Luther III, G.W., 2005. Basic processes of black sea biogeochemistry. Oceanography 18, 25–35.

Kostka, J.E., Luther III, G.W., Nealson, K.H., 1995. Chemical and biological reduction of Mn(III)-pyrophosphate complexes: potential importance of dissolved Mn(III) as an environmental oxidant. Geochim. Cosmochim. Acta 59, 885–894.

Kuypers, M.M., Sliekers, A.O., Lavik, G., Schmid, M., Jørgensen, B.B., Kuenen, J.G., Sinninghe Damsté, J.S., Strous, M., Jetten, M.S., 2003. Anaerobic ammonium oxidation by anammox bacteria in the Black Sea. Nature 442, 608–611.

Latif, M.A., Özsoy, E., Oğuz, T., Ünlüata, Ü., 1991. Observations of the Mediterranean inflow into the Black Sea. Deep-Sea Res. 38 (Suppl. 2), 711–723.

Ludwig, W., Bouwman, A.F., Dumont, E., Lespinas, F., 2010. Water and nutrient fluxes from major Mediterranean and Black Sea rivers: past and future trends and their implications for the basin-scale budgets. Global Biogeochem. Cycles 24, GB0A13.

Luther III, G.W., Church, T.M., Powel, D., 1991. Sulfur speciation and sulfide oxidation in the water column of the Black Sea. Deep-Sea Res. II 38, S1121–S1138.

Medinets, S., Medinets, V., 2012. Investigations of atmospheric wet and dry nutrient deposition to marine surface in western part of the Black Sea. Turkish J. Fish. Aquat. Sci. 12, 497–505.

Mee, L.D., 1992. The Black Sea in crisis: the need for concerted international action. Ambio 21 (4), 278–286.

Mee, L.D., Friedrich, J., Gomoiu, M.T., 2005. Restoring the Black Sea in times of uncertainty Oceanography. 18 (2), 100–111.

Murray, J.W., Izdar, E., 1989. The 1988 Black Sea Oceanographic Expedition: overview and new discoveries. Oceanography 2, 15–21.

Murray, J.W., Jannasch, H.W., Honjo, S., Anderson, R.F., Reeburg, W.S., Top, Z., Friederich, G.E., Codispoti, L.A., Izdar, E., 1989. Unexpected changes in the oxic/anoxic interface in the Black Sea. Nature 338, 411–413.

Murray, J.W., Top, Z., Ozsoy, E., 1991. Hydrographic properties and ventilation of the Black Sea. Deep-Sea Res. 38 (Suppl. 2), S663–S689.

Murray, J.M., Codispoti, L.A., Freiderich, G.E., 1995. Oxidation–reduction environments: the suboxic zone in the Black Sea. In: Huang, C.P., O'Melia, C.R., Morgan, J.J. (Eds.), Aquatic Chemistry, ACS Advances in Chemistry Series, 244, pp. 157–176.

Oguz, T., 2002. Role of physical processes controlling oxycline and suboxic layer structures in the Black Sea. Global Biogeochem. Cycles 16, 1–10.

Oguz, T., 2008. General oceanographic properties: physico-chemical and climatic features. In: Oguz, Temel (Ed.), State of the Environment of the Black Sea (2001–2006/7). Publications of the Commission on the Protection of the Black Sea against Pollution (BSC) 2008-3, Istanbul, Turkey (448 pp.).

Oguz, T., Ediger, D., 2006. Comparison of in situ and satellite-derived chlorophyll pigment concentrations, and impact of phytoplankton bloom on the suboxic layer structure in the western Black Sea during May–June 2001. Deep-Sea Res. II 53, 1923–1933.

Oguz, T., Velikova, V., 2010. Abrupt transition of the northwestern Black Sea shelf ecosystem from a eutrophic to an alternative pristine state. Mar. Ecol. Prog. Ser. 405, 231–242.

Oguz, T., La Violette, P., Unluata, U., 1992. Upper layer circulation of the southern Black Sea: its variability as inferred from hydrographic and satellite observations. J. Geophys. Res. 97 (C8), 12569–12584.

Oguz, T., Murray, J.W., Callahan, A., 2001. Modeling redox cycling across the suboxic–anoxic interface zone in the Black Sea. Deep-Sea Res. I 48, 761–787.

Oguz, T., Dippner, J.W., Kaymaz, Z., 2006. Climatic regulation of the Black Sea hydro-meteorological and ecological properties at interannual-to-decadal time scales. J. Mar. Syst. 60, 235–254.

Oguz, T., Velikova, V., Cociasu, A., Korchenko, A., 2008. The State of Eutrophication In: State of the Environment of the Black Sea (2001–2006/7). In: Oguz, Temel (Ed.), Publications of the Commission on the Protection of the Black Sea against Pollution (BSC) 2008-3, Istanbul, Turkey (448 pp.).

Ozsoy, E., Ünlüata, Ü., Top, Z., 1993. The evolution of Mediterranean water in the Black Sea; interior mixing and material transport by double diffusive intrusions. Prog. Oceanogr. 31 (3), 275–320.

Polat, Ç., Tugrul, S., 1995. Nutrient and organic carbon exchanges between the Black and Marmara seas through the Bosphorus Strait. Cont. Shelf Res. 15 (9), 1115–1132.

Polat, Ç., Tuğrul, S., Çoban, Y., Basturk, O., Salihoğlu, I., 1998. Elemental composition of seston and nutrient dynamics in the Sea of Marmara. Hydrobiologia 363, 157–167.

Shaffer, G., 1986. Phosphorus pumps and shuttles in the Black Sea. Nature 321, 515–517.

Sorokin, Y.I., 2002. The Black Sea — Ecology and Oceanography. Backhuys Publishers, UNESCO Venice Office, Leiden (875 pp.).

Spencer, D.W., Brewer, P.G., 1971. Vertical advection, diffusion and redox potentials as controls on the distribution of manganese and other trace metals dissolved in waters of the Black Sea. J. Geophys. Res. 76, 5877–5892.

Spencer, D.W., Brewer, P.G., Sachs, P.L., 1972. Aspects of the distribution and trace element composition of suspended matter in the Black Sea. Geochim. Cosmochim. Acta 36 (1), 71–86.

Stanev, E.V., Beckers, J.M., 1999. Numerical simulations of seasonal and interannual variability of the Black Sea thermohaline circulation. J. Mar. Syst. 22, 241–267.

Strokal, M., Kroeze, C., 2013. Nitrogen and phosphorus inputs to the Black Sea in 1970–2050. Reg. Environ. Chang. 13, 179–192. http://dx.doi.org/10.1007/s10113-012-0328-z.

Tolmazin, D., 1985. Changing coastal oceanography of the Black Sea. I. Northwestern shelf. Prog. Oceanogr. 15, 217–276.

Trouwborst, R.E., Clement, B.G., Tebo, B.M., Glazer, B.T., Luther III, G.W., 2006. Soluble Mn (II) in suboxic zones. Science 313, 1955–1957.

Tugrul, S., Basturk, Ö., Saydam, C., Yılmaz, A., 1992. Changes in the hydrochemistry of the Black Sea inferred from water density profiles. Nature 359, 137–139.

Vinogradov, M.Y., Nalbandov, Y.R., 1990. Effect of changes in water density on the profiles of physicochemical and biological characteristics in the pelagic ecosystem of the Black Sea. Oceanology 30, 567–573.

Yakushev, E.V., Pollehne, F., Jost, G., Kuznetsov, I., Schneider, B., Umlauf, L., 2007. Analysis of the water column oxic/anoxic interface in the Black and Baltic Seas with a numerical model. Mar. Chem. 107, 388–410.

Yakushev, E.V., Pakhomova, S., Sørenson, K., Skei, J., 2009. Importance of the different manganese species in the formation of water column redox zones: observations and modeling. Mar. Chem. 117, 59–70.

Yayla, M.K., Yılmaz, A., Morkoç, E., 2001. The dynamics of nutrient enrichment and primary production related to the recent changes in the ecosystem of the Black Sea. Aquat. Ecosyst. Heal. Manag. 4 (1), 31–49.

Yemenicioglu, S., Erdogan, S., Tugrul, S., 2006. Distributions of dissolved forms of iron and manganese in the Black Sea. Deep-Sea Res. II Trop. Stud.Oceanogr. 53 (17–19), 1842–1855.

Yiğiterhan, O., Murray, J.W., Tugrul, S., 2011. Trace metal composition of suspended particulate matter in the water column of the Black Sea. Mar. Chem. 126, 207–228.

Yılmaz, A., Tuğrul, S., Polat, Ç., Ediger, D., Çoban, Y., Morkoc, E., 1998. On the production, elemental composition (C, N, P) and distribution of photoautotrophic organic matter in the southern Black Sea. Hydrobiologia 363, 141–156.

Yılmaz, A., Tuğrul, Çoban-Yıldız Y., Karakoç, F., Bologa, A., 2006. Surface and mid-water sources of organic carbon by photoautotrophic and chemoautotrophic production. Deep-Sea Res. II 53, 1988–2004.

Yunev, O.A., Vedernikov, V.I., Baştурk, O., Yılmaz, A., Kıdeyş, A., Moncheva, S., Konovalov, S., 2002. Long-term variations of surface chlorophyll-a and primary production levels in the open Black Sea. Mar. Ecol. Prog. Ser. 230, 11–28.